



CERN-EP-2023-181
24 August 2023

Exploring the strong interaction of three-body systems at the LHC

ALICE Collaboration*

Abstract

Deuterons are atomic nuclei composed of a neutron and a proton held together by the strong interaction. Unbound ensembles composed of a deuteron and a third nucleon have been investigated in the past using scattering experiments and they constitute a fundamental reference in nuclear physics to constrain nuclear interactions and the properties of nuclei. In this work K^+ -d and p-d femtoscopic correlations measured by the ALICE Collaboration in proton-proton (pp) collisions at $\sqrt{s} = 13$ TeV at the Large Hadron Collider (LHC) are presented. It is demonstrated that correlations in momentum space between deuterons and kaons or protons allow us to study three-hadron systems at distances comparable with the proton radius. The analysis of the K^+ -d correlation shows that the relative distances at which deuterons and proton/kaons are produced are around 2 fm. The analysis of the p-d correlation shows that only a full three-body calculation that accounts for the internal structure of the deuteron can explain the data. In particular, the sensitivity of the observable to the short-range part of the interaction is demonstrated. These results indicate that correlations involving light nuclei in pp collisions at the LHC will also provide access to any three-body systems in the strange and charm sectors.

arXiv:2308.16120v1 [nucl-ex] 30 Aug 2023

© 2023 CERN for the benefit of the ALICE Collaboration.

Reproduction of this article or parts of it is allowed as specified in the CC-BY-4.0 license.

*See Appendix A for the list of Collaboration members

The study of many-body systems is a key aspect of modern nuclear physics because of its relevance for the structure of nuclear bound states [1–3] and for the equation of state of dense nuclear matter [4, 5]. Effects that go beyond the simple addition of the strong interaction between pairs of nucleons emerge already in the description of the most basic properties of light nuclei. Realistic potentials describing nucleon–nucleon interactions [6, 7] have therefore been complemented with phenomenological models of three-nucleon forces [8, 9]. In calculations using potentials derived from chiral effective field theories (EFTs) [2, 10], the many-body forces appear naturally as subleading terms in the chiral expansion. They find contributions of the order of 10% to the ground-state energies of $A \leq 12$ nuclei from genuine three-body nucleon forces [11, 12], and deliver predictions for heavier and neutron-rich nuclear structures.

In this context, two-nucleon scattering data and properties of the $A = 3$ systems are still the most important ingredients to constrain the parameters of nuclear interactions derived from EFT [13–15]. In particular, differential scattering observables for the p–d system have allowed for the computation of a full-fledged three-body wave function that accounts for all the relevant two- and three-body interactions at work in the p–(pn) system for the short and the asymptotic range [16–18]. In this work, it is demonstrated that such a standard candle of the three-body nuclear interaction can also be investigated by means of p–d correlations in momentum space measured at the LHC.

Momentum correlations of deuteron with other hadron species have already been considered as a tool to study both the deuteron production mechanism [19] and the final-state interactions for many-body systems. Different experimental correlations such as p–d and d–d have been measured [20–23] in O–Au reactions at $E/A = 25, 35, \text{ and } 60$ MeV and in ^{40}Ar – ^{58}Ni reactions at 77 MeV/u. The data showed a clear signature of the strong final-state interaction among light nuclei and nucleons, but the specific description of the process from a many-body perspective, as well as the tools to precisely measure the relative distances between particles, were not available at the time of those analyses.

Deuteron–hadron momentum correlations can also be investigated at the LHC, since light (anti)nuclei can be abundantly produced and accurately measured in ultra-relativistic nucleus-nucleus collisions [24–32]. Recent femtoscopy analyses carried out by ALICE in pp, p–Pb, and Pb–Pb collisions have demonstrated that it is possible to study the strong interaction among several hadron pairs [33–39] given the short distances at which hadrons can be produced in such colliding systems [40].

In this work, by means of a comprehensive study of the K^+ –d and p–d correlation functions measured in pp collisions at center-of-mass energy $\sqrt{s} = 13$ TeV with the ALICE detector at the LHC, evidence is provided that deuterons are formed at distances of the order of 2 fm from other hadrons. The measurement of the p–d correlation at such short distances constitutes an innovative method to study three-body systems at the LHC, with the potential of extending such studies to the strangeness and charm sector. Indeed, in the strangeness sector, a similar approach as the one adopted for standard nuclear physics is envisaged for the future by improving the database of hypernuclei [41–43], scattering experiments [44], and femtoscopy measurements in hadron–hadron collisions [45, 46]. Direct measurements of the hyperon–deuteron systems at short distances would provide complementary information to these standard methods.

Correlation function from scattering parameters

Final-state interactions involving light nuclei such as deuterons have been studied in the past via scattering experiments [47–51]. In scattering theory, the nuclear interaction in the asymptotic regime, can be investigated by associating a plane wave to the incoming particle and building the outgoing wave as a superposition of spherical waves with phase shifts δ_l , with l denoting the relative angular momentum between the projectile and the target. The interaction determines the values of δ_l , and for $l = 0$, referred to as s -wave scattering, a scattering length a_0 , is commonly used to characterize the interaction at zero energy and can be related to the differential cross section measured in scattering experiments. These

measurements enable also the determination of the effective range of the interaction, d_0 .

Scattering experiments have been already performed for the K^+ -d and p-d systems allowing for the extraction of the corresponding scattering parameters, as reported in Table 1. In the case of K^+ -d, such parameters are spin averaged and they are calculated with two different methods: i) via an effective range fit (ER) to the cross section predictions at threshold anchored to the available scattering data [52]; ii) from the well-known K-N interactions [53] using the fixed-center approximation (FCA) [54]. The negative values of the K^+ -d scattering length (a_0) refer to a repulsive strong interaction. In the case of the p-d system, the parameters for the spin doublet ($S = 1/2$) and quartet ($S = 3/2$) channels were obtained by using theoretical calculations [55–59] and a vast collection of scattering data [47–51]. The positive sign of the p-d scattering parameters reported in Table 1 corresponds to a repulsive interaction for the quartet state ($S = 3/2$), but for the doublet state ($S = 1/2$), the ^3He bound state emerges, and the standard effective range expansion has to be modified (see Eq. 2 in [58]).

Table 1: Scattering lengths a_0 and effective ranges d_0 for the p-d and K^+ -d s -wave states. For the p-d, the two spin states (doublet and quartet) are reported. For the meson-baryon system, negative values of scattering length refer to a repulsive interaction. For the baryon-baryon system, negative and positive values of a_0 refer to attractive and repulsive interactions (for cases where the potential does not support two-body bound states), respectively.

System	Spin averaged		$S = 1/2$		$S = 3/2$		References
	$a_0(\text{fm})$	$d_0(\text{fm})$	$a_0(\text{fm})$	$d_0(\text{fm})$	$a_0(\text{fm})$	$d_0(\text{fm})$	
K^+ -d	-0.470	1.75	—	—	—	—	ER [52]
	-0.540	0.0	—	—	—	—	FCA [53, 54]
p-d			$2.73^{+0.10}_{-0.10}$	$2.27^{+0.12}_{-0.12}$	$11.88^{+0.10}_{-0.40}$	$2.63^{+0.01}_{-0.02}$	Arvieux [55]
			$1.30^{+0.20}_{-0.20}$	—	$11.40^{+1.80}_{-1.20}$	$2.05^{+0.25}_{-0.25}$	VanOers [56]
			4.0	—	11.1	—	Huttel [57]
			0.024	—	13.8	—	Kievsky [58]
			$-0.13^{+0.04}_{-0.04}$	—	$14.70^{+2.30}_{-2.30}$	—	Black [59]

An alternative method to test the accuracy of the relative wave function in a two-hadron system is the measurement of the correlation function among the pairs of interest produced in hadron-hadron collisions [36]. The theoretical correlation function can be expressed [60, 61] as $C(k^*) = \int d^3r^* S(r^*) |\psi(\vec{k}^*, \vec{r}^*)|^2$, where $S(r^*)$ is the distribution of the distance r^* between the emitted particles in a hadron-hadron collision, defining the particle source; $\psi(\vec{k}^*, \vec{r}^*)$ represents the wave function of the relative motion for the pair of interest and k^* is the reduced relative momentum of the pair ($k^* = |\vec{p}_2^* - \vec{p}_1^*|/2$). The asterisk indicates that the quantities are evaluated in the pair rest frame, where $p_1^* = -p_2^*$. The Lednický-Lyuboshitz (LL) formalism [62, 63] provides a simplified analytical treatment of the wave function (see Methods for details), that can relate the correlation function to its asymptotic behavior where the core nuclear strong interaction is not considered. The analytical formula for the correlation function is obtained assuming a Gaussian source distribution in r^* , and a single set of scattering parameters. The formula is averaged over spin and isospin and only considers s -waves in the scattering process.

Experimentally, the correlation function is defined as $C(k^*) = \xi(k^*) \otimes \frac{N_{\text{same}}(k^*)}{N_{\text{mixed}}(k^*)}$, where $\xi(k^*)$ denotes the corrections for experimental effects (see Methods for details), $N_{\text{same}}(k^*)$ is the number of detected particle pairs in a given k^* interval obtained by combining particles produced in the same collision (event), which constitute a sample of correlated pairs, and $N_{\text{mixed}}(k^*)$ is the number of uncorrelated pairs in the same k^* interval, obtained by combining particles produced in different collisions (mixed events). In this work, the interest resides in studying the final-state interaction for K^+ -d and p-d pairs produced

in pp collisions at $\sqrt{s} = 13$ TeV. The analyzed data set was collected using an online trigger to select high-multiplicity pp collisions to enhance the pair sample size. Kaon (K^+), antikaon (K^-), proton (p), antiproton (\bar{p}), deuteron (d), and antideuteron (\bar{d}) tracks are reconstructed with the ALICE detector and their momentum in the laboratory frame p is measured in the range $p \in [0.2, 4.1]$ GeV/c. The particle identification is carried out using measurements of the specific energy loss in Time Projection Chamber (TPC) and time of flight (TOF detector), resulting in samples of K^+ (K^-), p (\bar{p}), d (\bar{d}) with a purity of 99.8 (99.8)%, 98.2 (97.9)%, and 100 (100)% respectively, as estimated via Monte Carlo simulations. Details on the experimental methods and the evaluation of the systematic uncertainties are described in Methods. Once the kaons, protons, and deuterons (and charge conjugates) are selected and their three-momenta measured, the correlation functions can be built. Since it is assumed that the same interaction governs hadron–hadron and antihadron–antihadron pairs [33], in the following, the sum of particles and antiparticles is considered ($K^+-d \equiv K^+-d \oplus K^--\bar{d}$ and $p-d \equiv p-d \oplus \bar{p}-\bar{d}$).

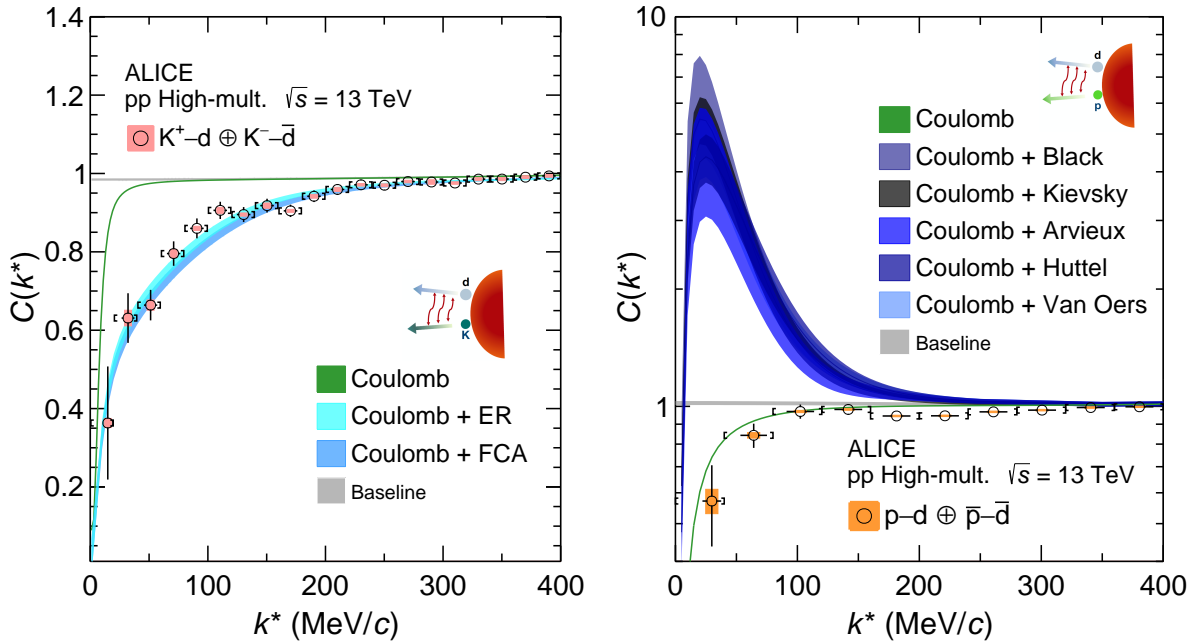


Figure 1: Measured K^+-d (left) and $p-d$ (right) correlation functions. The data are shown by the black symbols, the bars and the colored boxes represent the statistical and systematic uncertainties, respectively. The square brackets show the bin width of the measurement, while the horizontal black lines represent the statistical uncertainty in the determination of the mean k^* for each bin. Data are compared with theoretical correlation functions, shown by colored bands, obtained using the LL approximation. The bandwidths represent the uncertainties in the determination of the radius and the residual contributions. See text for details.

Figure 1 shows the K^+-d (left panel) and $p-d$ (right panel) correlation functions as a function of k^* measured in pp collisions at $\sqrt{s} = 13$ TeV with ALICE. Both correlation functions are below unity for values of k^* smaller than 200 MeV/c, indicating an overall repulsive interaction. The measured correlation functions are compared to calculations performed using the LL approximation considering either only the Coulomb interaction or, in addition, the strong interaction part determined by the scattering parameters reported in Table 1 for the K^+-d and $p-d$ systems. In order to compare the experimental data to the LL calculations, the source term included in the formula of the correlation function and the feed-down corrections due to particle decays and residual background contributions are needed to match the experimental measurements.

The source term has been approximated as a Gaussian distribution, whose width, defining the source size, need to be evaluated. The values of the $p-d$ and K^+-d source sizes have been obtained from the results of independent analyses of $p-p$ correlations, which demonstrate the existence of a universal source for

any hadron–hadron pair in pp collisions at the LHC [40] and indicate that the source size decreases with an increasing value of the pair transverse mass m_T (see Methods). In addition, further modifications of the source distribution due to strong decays of short-lived resonances decaying into protons and kaons are taken into account. For p–d pairs an effective source size of $r_{\text{eff}}^{\text{p-d}} = 1.08 \pm 0.06$ fm is obtained. For the K^+ –d pairs the contribution of broad resonances with very different decay times has been taken into account and the effective source results in $r_{\text{eff}}^{\text{K}^+\text{-d}} = 1.35^{+0.04}_{-0.05}$ fm. Note that such small source sizes imply that the most probable distance between particles is around 2 fm [64].

The calculated correlation functions using the LL method, shown by the colored bands in Fig. 1 have been corrected for feed-down from weak and strong decays and residual background contributions, using the data-driven methods described in [33] and [65], respectively. The relative contributions from primarily produced K^+ –d and p–d pairs to the corresponding inclusive sample are obtained experimentally and are 0.92 and 0.82, respectively. The residual background contribution is shown as the grey-colored band close to the unity. The width of the theoretical bands stems from the uncertainty propagation of the experimental determination of the source size, feed-down, and residual background. Additional information on the source size and the different contributions to the correlation function is provided in Methods.

The measured K^+ –d correlation function is lower than the Coulomb-only prediction showing the presence of a repulsive strong interaction. The calculations with the LL approximation using both sets of scattering parameters (ER and FCA) provide an excellent description of the experimental correlation function within uncertainties. Indeed, since both the Coulomb and strong K^+ –d interactions are repulsive and there is no short-range structure in this interaction, an asymptotic description is sufficient to describe the data. Additionally, kaons are bosons and the proton and neutron that constitute the deuteron are fermions, hence the LL approximation of point-like and distinguishable particles is pertinent and the properties of the deuteron are mapped in the K^+ –d scattering parameters. The agreement between the model and the data, obtained for the small radius ($r_{\text{eff}}^{\text{K}^+\text{-d}} = 1.35^{+0.04}_{-0.05}$ fm) that follows the same m_T scaling as all other hadron pairs, shows that deuterons are produced at small distances with respect to other hadrons in pp collisions at the LHC and this result provides an excellent reference for the source term of correlations involving deuterons.

Instead, a huge discrepancy is observed when comparing the p–d data to analogous calculations which consider protons and deuterons as distinguishable point-like particles and employing the small source size obtained from the m_T scaling. This can be seen by comparing the measured p–d correlation in the right panel of Fig. 1 to the five different blue shaded curves which are obtained using the five sets of scattering lengths reported in Table 1.

The limitations of the LL approximation in describing in detail the p–d interaction are several. The existence of the ^3He bound state introduces a particular short-range behavior in the doublet state due to orthogonality requirements. Moreover, the spin structure of the quartet state is completely symmetric implying as well a specific short-range behavior of the corresponding spatial part to fulfill the requirements of the Pauli principle. In addition, the correct antisymmetrization of the wave function is not considered in the LL approximation, and such short-range features of the interactions are not taken into account. On the other hand, the correlation function obtained with the Coulomb-only assumption (green curve in the right panel of Fig. 1) catches the correct amplitude of the experimental p–d correlation function despite the sizable scattering parameters reported in Table 1. This apparent mismatch is due to the fact that in this case, the Coulomb repulsion between the proton and the deuteron reduces the impact of the short-range part of the wave function in the correlation function, and the three-fermion system is not correctly treated within the LL approximation even if only the Coulomb interaction is considered.

Correlation function of a three-body system

In order to correctly describe the three-body system p –(pn) the microscopic p – d wave function must be employed in the calculation of the p – d correlation function. The latter has been obtained by projecting the p – d wave functions on the initial three-nucleon state created after the pp collisions. The relevant source term in this calculation depends on an effective nucleon–nucleon source radius $r_{\text{eff}}^{\text{NN}}$ [66, 67], since the single nucleons are the relevant degrees of freedom. Details of the calculation are presented in Methods and in [68].

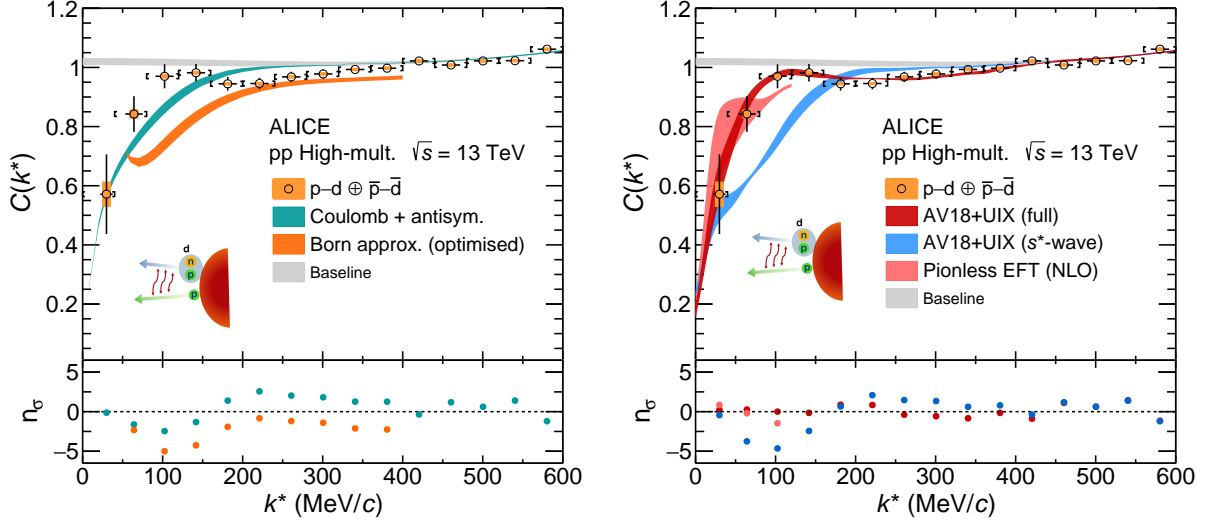


Figure 2: Measured p – d correlation function plotted as a function of the p – d relative momentum k^* alongside theoretical calculations. The experimental data are represented by circular symbols. The black vertical bars and orange boxes correspond to the statistical and systematic uncertainties, respectively. The square brackets indicate the measurement bin width and the horizontal black lines represent the statistical uncertainty in the determination of the mean k^* for each bin. The non-femtoscopic background contributions are represented by the gray band of the cubic baseline. Left panel: the orange and turquoise bands depict calculations obtained using an optimized Born approximation and Coulomb + antisymmetrization of the three-particle wave function, respectively. Right panel: the dark red band represents a fit of the modeled correlation calculated considering p – d as a three-body system with all relevant partial waves. The blue-colored band corresponds to a calculation that includes only the s -wave contribution. The light red band represents a calculation of the correlation function using Pionless EFT at NLO (see text). All calculations are multiplied by the cubic baseline, and the bandwidths of all calculations account for uncertainties in the determination of the radius and residual contributions. The lower panels present the difference between the measured and calculated correlation function, expressed as the number of standard deviations, n_σ , taking into account the statistical uncertainties of the data and the model uncertainties.

Three different versions of the p – d wave function have been investigated to study the microscopic behavior of the p – d system. First, a Born approximation of the p – d wave function that contains the correct antisymmetrization for the p –(pn) system but where the short-range contribution of the wave function has been omitted. Hence, this calculation accounts only for the asymptotic part of the wave function similar to the LL model but considers the microscopic structure of the p – d system.

The left panel of Fig. 2 shows how the Born approximation compares to the experimental data, including n_σ values that quantify the data-model deviation. It can be seen that this calculation is not sufficiently accurate to reproduce the data, although the antisymmetrization is correctly accounted for. For k^* below 60 MeV/ c , this calculation predicts non-physical values and therefore they are excluded from the figure. In the same panel, the comparison to the full-fledged Coulomb-only calculation considering the dynamics

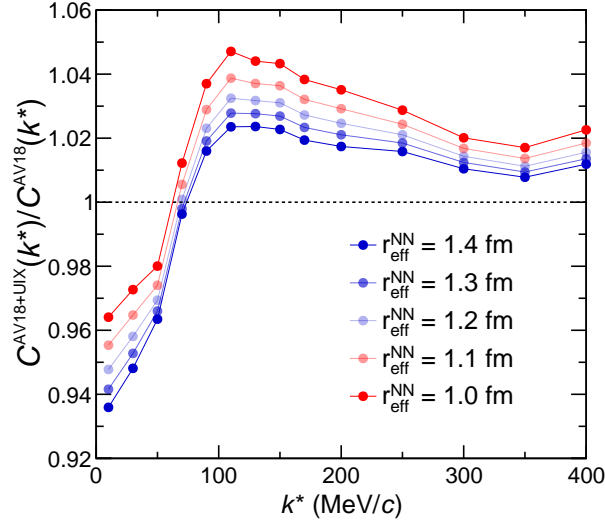


Figure 3: Ratio of theoretical p–d correlation functions obtained with full three-body calculations (AV18 for NN + UIX for NNN interaction) to those obtained using an AV18 for NN interaction only for different values of the two-nucleon effective source size $r_{\text{eff}}^{\text{NN}}$.

of three nucleons in the p–d system is shown as well, indicating also a clear disagreement with the data.

The second wave function that has been tested has been obtained employing the Hyperspherical Harmonics (HH) method [16]. It accounts for all the relevant two- and three-body interactions at work in the p–(pn) system for the short and the asymptotic range, it accurately describes the three-body dynamics, and it is calculated using p–d scattering observables [16–18]. The nuclear interaction includes the AV18 two-nucleon (NN) [6] plus the Urbana IX (UIX) three-nucleon (NNN) [8] and the Coulomb potentials. The blue curve in the right panel of Fig. 2 has been obtained by including the NN and NNN interactions only in the $J^\pi = \frac{1}{2}^+, \frac{3}{2}^+$ partial waves relative to the p–d system, which are dominated by the *s*-wave contributions [68]. The n_σ distribution in the lower panel shows that the calculation with even partial waves describes the data moderately well but fails in the small relative momentum part. The agreement improves when more partial waves up to $J^\pi = \frac{7}{2}^-$ are included in the calculation, where the *p*-waves contribute predominantly, as it is shown by the red curve of the right panel of Fig. 2. The full calculation has been fitted to the experimental data allowing for a multiplicative baseline (gray curve in Fig. 2) as a residual background. The same background has been used for the comparison of the other calculations, and the curves’ widths represent the propagated uncertainty of the source parameter and baseline. The full calculation describes the experimental data very accurately, as indicated by the n_σ values for the red band remaining consistently close to or below one across the entire range of k^* .

As an additional check, the light red band in the right panel of Fig. 2 shows the p–d correlation function calculated in pionless effective field theory [69] (Pionless EFT) calculation at next-to-leading order (NLO). The nuclear interaction within this approach is much simpler than the AV18+UIX potential [68]; the NN interaction is determined by only the *s*-wave NN scattering lengths and effective ranges up to NLO, while the NNN interaction is fixed by either the ^3H binding energy or the n–d *s*-wave scattering length. For the Pionless EFT calculation, the additional uncertainty from truncating the EFT expansion at NLO can be estimated as 10%. Taking this into account, in the regime where the theory is applicable (k^* below the pion mass ~ 140 MeV/*c*), the Pionless EFT results are largely compatible with the HH calculation using the AV18+UIX force.

The fact that the experimental p–d correlation function can only be described by a full-fledged calculation of a three-body system that considers the single nucleons as active degrees of freedom and that the shape of the correlation function is also sensitive to the inclusion of different partial waves in the interaction

demonstrates for the first time that deuteron–proton correlations measured in pp collisions at the LHC access the three-nucleon system at short distances. Indeed, past measurements of correlations involving deuterons [20–23] have been interpreted by means of the LL calculation combined with a value of the source radius larger than the one found for other hadron–hadron pairs in the same colliding system. This misinterpretation of the data was caused by the lack of correct microscopic calculations of the p–d system.

In order to test the sensitivity of the p–d correlation function to genuine three-baryon interactions, the full-fledged p–d calculation has been carried out excluding such interactions [68]. Figure 3 shows the ratio of the calculated p–d correlation with the AV18+UIX interactions to the calculation including only the AV18 NN interactions evaluated for different values of the two-nucleon source size $r_{\text{eff}}^{\text{NN}}$. The current precision of the data does not allow for testing such effects. However, this will be possible on the larger data samples that will be collected during the LHC Run 3 (2022–2025) with the ALICE upgraded apparatus [70]. The integrated luminosity will be increased by one order of magnitude with respect to the dataset used in the current work [71], enabling the study of the interaction at small distances by triggering on p–d pairs with large m_T values. Such studies can also be extended to systems such Λ/Σ –d or Λ_c^+ –d to investigate three-baryon systems in the strange and charm sectors which are otherwise inaccessible.

Acknowledgements

The ALICE Collaboration is grateful to Prof. Johann Haidenbauer and Prof. Tetsuo Hyodo for providing the derivation of the K^+ –d scattering parameters, and to Stanisław Mrówczyński and Urs Wiedemann for fruitful discussions.

The ALICE Collaboration would like to thank all its engineers and technicians for their invaluable contributions to the construction of the experiment and the CERN accelerator teams for the outstanding performance of the LHC complex. The ALICE Collaboration gratefully acknowledges the resources and support provided by all Grid centres and the Worldwide LHC Computing Grid (WLCG) collaboration. The ALICE Collaboration acknowledges the following funding agencies for their support in building and running the ALICE detector: A. I. Alikhanyan National Science Laboratory (Yerevan Physics Institute) Foundation (ANSL), State Committee of Science and World Federation of Scientists (WFS), Armenia; Austrian Academy of Sciences, Austrian Science Fund (FWF): [M 2467-N36] and Nationalstiftung für Forschung, Technologie und Entwicklung, Austria; Ministry of Communications and High Technologies, National Nuclear Research Center, Azerbaijan; Conselho Nacional de Desenvolvimento Científico e Tecnológico (CNPq), Financiadora de Estudos e Projetos (Finep), Fundação de Amparo à Pesquisa do Estado de São Paulo (FAPESP) and Universidade Federal do Rio Grande do Sul (UFRGS), Brazil; Bulgarian Ministry of Education and Science, within the National Roadmap for Research Infrastructures 2020–2027 (object CERN), Bulgaria; Ministry of Education of China (MOEC), Ministry of Science & Technology of China (MSTC) and National Natural Science Foundation of China (NSFC), China; Ministry of Science and Education and Croatian Science Foundation, Croatia; Centro de Aplicaciones Tecnológicas y Desarrollo Nuclear (CEADEN), Cubaenergía, Cuba; Ministry of Education, Youth and Sports of the Czech Republic, Czech Republic; The Danish Council for Independent Research | Natural Sciences, the VILLUM FONDEN and Danish National Research Foundation (DNRF), Denmark; Helsinki Institute of Physics (HIP), Finland; Commissariat à l’Energie Atomique (CEA) and Institut National de Physique Nucléaire et de Physique des Particules (IN2P3) and Centre National de la Recherche Scientifique (CNRS), France; Bundesministerium für Bildung und Forschung (BMBF) and GSI Helmholtzzentrum für Schwerionenforschung GmbH, Germany; General Secretariat for Research and Technology, Ministry of Education, Research and Religions, Greece; National Research, Development and Innovation Office, Hungary; Department of Atomic Energy Government of India (DAE), Department of Science and Technology, Government of India (DST), University Grants Commission, Government of India (UGC) and Council of Scientific and Industrial Research (CSIR), India; National

Research and Innovation Agency - BRIN, Indonesia; Istituto Nazionale di Fisica Nucleare (INFN), Italy; Japanese Ministry of Education, Culture, Sports, Science and Technology (MEXT) and Japan Society for the Promotion of Science (JSPS) KAKENHI, Japan; Consejo Nacional de Ciencia (CONACYT) y Tecnología, through Fondo de Cooperación Internacional en Ciencia y Tecnología (FONCICYT) and Dirección General de Asuntos del Personal Académico (DGAPA), Mexico; Nederlandse Organisatie voor Wetenschappelijk Onderzoek (NWO), Netherlands; The Research Council of Norway, Norway; Commission on Science and Technology for Sustainable Development in the South (COMSATS), Pakistan; Pontificia Universidad Católica del Perú, Peru; Ministry of Education and Science, National Science Centre and WUT ID-UB, Poland; Korea Institute of Science and Technology Information and National Research Foundation of Korea (NRF), Republic of Korea; Ministry of Education and Scientific Research, Institute of Atomic Physics, Ministry of Research and Innovation and Institute of Atomic Physics and University Politehnica of Bucharest, Romania; Ministry of Education, Science, Research and Sport of the Slovak Republic, Slovakia; National Research Foundation of South Africa, South Africa; Swedish Research Council (VR) and Knut & Alice Wallenberg Foundation (KAW), Sweden; European Organization for Nuclear Research, Switzerland; Suranaree University of Technology (SUT), National Science and Technology Development Agency (NSTDA), Thailand Science Research and Innovation (TSRI) and National Science, Research and Innovation Fund (NSRF), Thailand; Turkish Energy, Nuclear and Mineral Research Agency (TENMAK), Turkey; National Academy of Sciences of Ukraine, Ukraine; Science and Technology Facilities Council (STFC), United Kingdom; National Science Foundation of the United States of America (NSF) and United States Department of Energy, Office of Nuclear Physics (DOE NP), United States of America. In addition, individual groups or members have received support from: European Research Council, Strong 2020 - Horizon 2020 (grant nos. 950692, 824093), European Union; Academy of Finland (Center of Excellence in Quark Matter) (grant nos. 346327, 346328), Finland; National Science Foundation, Grant No. PHY-2044632; U.S. Department of Energy, Office of Science, Office of Nuclear Physics, under the FRIB Theory Alliance, award DE-SC0013617.

References

- [1] H.-W. Hammer, A. Nogga, and A. Schwenk, “Three-body forces: from cold atoms to nuclei”, *Rev. Mod. Phys.* **85** (2013) 197, arXiv:1210.4273 [nucl-th].
- [2] H. Hergert, “A Guided Tour of *ab initio* Nuclear Many-Body Theory”, *Front. in Phys.* **8** (2020) 379, arXiv:2008.05061 [nucl-th].
- [3] J. Lynn, I. Tews, S. Gandolfi, and A. Lovato, “Quantum monte carlo methods in nuclear physics: Recent advances”, *Ann. Rev. Nucl. Part. Sci.* **69** (2019) 279–305.
- [4] M. Baldo, G. F. Burgio, and I. Bombaci, “Microscopic nuclear equation of state with three-body forces and neutron star structure”, *A&A* **328** (1997) 274–282, arXiv:nucl-th/9607013.
- [5] I. Bombaci and D. Logoteta, “Equation of state of dense nuclear matter and neutron star structure from nuclear chiral interactions”, *A&A* **609** (2018) A128.
- [6] R. B. Wiringa, V. G. J. Stoks, and R. Schiavilla, “Accurate nucleon-nucleon potential with charge-independence breaking”, *Phys. Rev. C* **51** (1995) 38–51.
- [7] V. G. J. Stoks, R. A. M. Klomp, C. P. F. Terheggen, and J. J. de Swart, “Construction of high quality N–N potential models”, *Phys. Rev. C* **49** (1994) 2950–2962, arXiv:nucl-th/9406039.
- [8] B. S. Pudliner et al, “Quantum Monte Carlo calculations of nuclei with $A \leq 7$ ”, *Phys. Rev. C* **56** (1997) 1720–1750, arXiv:nucl-th/9705009.
- [9] S. A. Coon and H. K. Han, “Reworking the Tucson-Melbourne three nucleon potential”, *Few Body Syst.* **30** (2001) 131–141, arXiv:nucl-th/0101003.

- [10] E. Epelbaum, H. Krebs, and P. Reinert, “High-precision nuclear forces from chiral EFT: State-of-the-art, challenges and outlook”, *Front. in Phys.* **8** (2020) 98, arXiv:1911.11875 [nucl-th].
- [11] **LENPIC** Collaboration, E. Epelbaum *et al.*, “Few- and many-nucleon systems with semilocal coordinate-space regularized chiral two- and three-body forces”, *Phys. Rev. C* **99** (2019) 024313, arXiv:1807.02848 [nucl-th].
- [12] M. Piarulli *et al.*, “Light-nuclei spectra from chiral dynamics”, *Phys. Rev. Lett.* **120** (2018) 052503, arXiv:1707.02883 [nucl-th].
- [13] M. Piarulli *et al.*, “Local chiral potentials with Δ -intermediate states and the structure of light nuclei”, *Phys. Rev. C* **94** (2016) 054007, arXiv:1606.06335 [nucl-th].
- [14] P. Reinert, H. Krebs, and E. Epelbaum, “Semilocal momentum-space regularized chiral two-nucleon potentials up to fifth order”, *Eur. Phys. J. A* **54** (2018) 86, arXiv:1711.08821 [nucl-th].
- [15] S. K. Saha, D. R. Entem, R. Machleidt, and Y. Nosyk, “Local position-space two-nucleon potentials from leading to fourth order of chiral effective field theory”, *Phys. Rev. C* **107** (2023) 034002.
- [16] A. Kievsky, M. Viviani, and S. Rosati, “Polarization observables in p-d scattering below 30 MeV”, *Phys. Rev. C* **64** (2001) 024002, arXiv:nucl-th/0103058.
- [17] A. Kievsky, M. Viviani, and L. E. Marcucci, “N-d scattering including electromagnetic forces”, *Phys. Rev. C* **69** (Jan, 2004) 014002.
- [18] A. Deltuva, A. C. Fonseca, A. Kievsky, S. Rosati, P. U. Sauer, and M. Viviani, “Benchmark calculation for proton-deuteron elastic scattering observables including Coulomb”, *Phys. Rev. C* **71** (2005) 064003, arXiv:nucl-th/0503015.
- [19] S. Mrówczyński and P. Słoń, “Hadron-deuteron correlations and production of light nuclei in relativistic heavy-ion collisions”, *Acta Phys. Polon. B* **51** (2020) 1739–1755, arXiv:1904.08320 [nucl-th].
- [20] C. B. Chitwood *et al.*, “Final-State interactions between noncompound light particles for ^{16}O -induced reactions on ^{197}Au at $E/A = 25$ MeV”, *Phys. Rev. Lett.* **54** (1985) 302–305.
- [21] J. Pochodzalla *et al.*, “External Coulomb distortion of proton-deuteron final-state interactions for induced reactions on Au at $E/A = 35$ MeV”, *Phys. Lett. B* **175** (1986) 275–278.
- [22] J. Pochodzalla *et al.*, “Two-particle correlations at small relative momenta for ^{40}Ar -induced reactions on ^{197}Au at $E/A = 60$ MeV”, *Phys. Rev. C* **35** (1987) 1695–1719.
- [23] K. Wosińska *et al.*, “Correlations of neutral and charged particles in ^{40}Ar - ^{58}Ni reaction at 77 MeV/u. *Eur. Phys. J. A* **32**, 55–59 (2007)”, *Eur. Phys. J. A.* **32** (2007) 55–59.
- [24] V. T. Cocconi, T. Fazzini, G. Fidecaro, M. Legros, N. H. Lipman, and A. W. Merrison, “Mass Analysis of the Secondary Particles Produced by the 25-GeV Proton Beam of the Cern Proton Synchrotron”, *Phys. Rev. Lett.* **5** (1960) 19–21.
- [25] S. Nagamiya, “Experimental overview”, *Nucl. Phys. A* **544** (1992) 5C–26C.
- [26] **STAR** Collaboration, C. Adler *et al.*, “Anti-deuteron and anti-He-3 production in $\sqrt{s_{\text{NN}}} = 130$ GeV Au+Au collisions”, *Phys. Rev. Lett.* **87** (2001) 262301, arXiv:nucl-ex/0108022. [Erratum: *Phys.Rev.Lett.* **87**, 279902 (2001)].

- [27] **PHENIX** Collaboration, S. S. Adler *et al.*, “Deuteron and antideuteron production in Au + Au collisions at $\sqrt{s_{NN}} = 200$ GeV”, *Phys. Rev. Lett.* **94** (2005) 122302, arXiv:nuc1-ex/0406004.
- [28] **STAR** Collaboration, H. Agakishiev *et al.*, “Observation of the antimatter helium-4 nucleus”, *Nature* **473** (2011) 353, arXiv:1103.3312 [nuc1-ex]. [Erratum: *Nature* 475, 412 (2011)].
- [29] **ALICE** Collaboration, S. Acharya *et al.*, “Production of deuterons, tritons, ^3He nuclei and their antinuclei in pp collisions at $\sqrt{s} = 0.9, 2.76$ and 7 TeV”, *Phys. Rev.* **C97** (2018) 024615, arXiv:1709.08522 [nuc1-ex].
- [30] **ALICE** Collaboration, J. Adam *et al.*, “Production of light nuclei and anti-nuclei in pp and Pb-Pb collisions at energies available at the CERN Large Hadron Collider”, *Phys. Rev. C* **93** (2016) 024917, arXiv:1506.08951 [nuc1-ex].
- [31] **ALICE** Collaboration, S. Acharya *et al.*, “(Anti-)deuteron production in pp collisions at $\sqrt{s} = 13$ TeV”, *Eur. Phys. J. C* **80** (2020) 889, arXiv:2003.03184 [nuc1-ex].
- [32] **ALICE** Collaboration, S. Acharya *et al.*, “Measurement of deuteron spectra and elliptic flow in Pb-Pb collisions at $\sqrt{s_{NN}} = 2.76$ TeV at the LHC”, *Eur. Phys. J. C* **77** (2017) 658, arXiv:1707.07304 [nuc1-ex].
- [33] **ALICE** Collaboration, S. Acharya *et al.*, “p-p, p- Λ and Λ - Λ correlations studied via femtoscopy in pp reactions at $\sqrt{s} = 7$ TeV”, *Phys. Rev. C* **99** (2019) 024001, arXiv:1805.12455 [nuc1-ex].
- [34] **ALICE** Collaboration, S. Acharya *et al.*, “First observation of an attractive interaction between a proton and a cascade baryon”, *Phys. Rev. Lett.* **123** (2019) 112002, arXiv:1904.12198 [nuc1-ex].
- [35] **ALICE** Collaboration, S. Acharya *et al.*, “Scattering studies with low-energy kaon-proton femtoscopy in proton-proton collisions at the LHC”, *Phys. Rev. Lett.* **124** (2020) 092301, arXiv:1905.13470 [nuc1-ex].
- [36] **ALICE** Collaboration, S. Acharya *et al.*, “Unveiling the strong interaction among hadrons at the LHC”, *Nature* **588** (2020) 232–238, arXiv:2005.11495.
- [37] **ALICE** Collaboration, S. Acharya *et al.*, “Experimental evidence for an attractive p- ϕ interaction”, *Phys. Rev. Lett.* **127** (2021) 172301, arXiv:2105.05578 [nuc1-ex].
- [38] **ALICE** Collaboration, S. Acharya *et al.*, “First study of the two-body scattering involving charm hadrons”, *Phys. Rev. D* **106** (2022) 052010, arXiv:2201.05352 [nuc1-ex].
- [39] **ALICE** Collaboration, S. Acharya *et al.*, “Kaon-proton strong interaction at low relative momentum via femtoscopy in Pb-Pb collisions at the LHC”, *Phys. Lett. B* **822** (2021) 136708, arXiv:2105.05683 [nuc1-ex].
- [40] **ALICE** Collaboration, S. Acharya *et al.*, “Search for a common baryon source in high-multiplicity pp collisions at the LHC”, *Phys. Lett. B* **811** (2020) 135849.
- [41] A. Feliciello and T. Nagae, “Experimental review of hypernuclear physics: recent achievements and future perspectives”, *Rept. Prog. Phys.* **78** (2015) 096301.
- [42] L. Tolos and L. Fabbietti, “Strangeness in nuclei and neutron stars”, *Prog. Part. Nucl. Phys.* **112** (2020) 103770, arXiv:2002.09223 [nuc1-ex].
- [43] T. R. Saito *et al.*, “New directions in hypernuclear physics”, *Nature Rev. Phys.* **3** (2021) 803–813.

- [44] CLAS Collaboration, J. Rowley *et al.*, “Improved Λp elastic scattering cross sections between 0.9 and 2.0 GeV/c as a main ingredient of the neutron star equation of state”, *Phys. Rev. Lett.* **127** (Dec, 2021) 272303.
- [45] L. Fabbietti, V. Mantovani Sarti, and O. Vazquez Doce, “Study of the strong interaction among hadrons with correlations at the LHC”, *Ann. Rev. Nucl. Part. Sci.* **71** (2021) 377–402, arXiv:2012.09806 [nucl-ex].
- [46] ALICE Collaboration, “The ALICE experiment – A journey through QCD”, (*submitted to EPJC*) (2022), arXiv:/2211.04384v1 [nucl-ex].
- [47] L. D. Knutson *et al.*, “Determination of the phase shifts for p–d elastic scattering at $E_p = 3$ MeV”, *Phys. Rev. Lett.* **71** (Dec, 1993) 3762–3765.
- [48] R. Sherr *et al.*, “Scattering of protons by deuterons”, *Phys. Rev.* **72** (Oct, 1947) 662–672.
- [49] C. Brune *et al.*, “Possible three-nucleon force effects in d–p scattering at low energies”, *Phys. Lett. B* **428** (1998) 13–17.
- [50] E. Huttel, W. Arnold, H. Berg, H. Krause, J. Ulbricht, and G. Clausnitzer, “Differential cross sections and analyzing powers for pd elastic scattering below 1.0 MeV”, *Nucl. Phys. A* **406** (1983) 435–442.
- [51] T. Clegg *et al.*, “A new atomic beam polarized ion source for the triangle universities nuclear laboratory: overview, operating experience, and performance”, *Nucl. Instrum. Methods Phys. Res.* **357** (1995) 200–211.
- [52] T. Takaki, “Optical Potential Approach to K^+ d Scattering at Low Energies”, *Phys. Rev. C* **81** (2010) 055204, arXiv:0911.5480 [nucl-th].
- [53] K. Aoki and D. Jido, “KN scattering amplitude revisited in a chiral unitary approach and a possible broad resonance in $S = +1$ channel”, *PTEP* **2019** (2019) 013D01, arXiv:1806.00925 [nucl-th].
- [54] S. S. Kamalov, E. Oset, and A. Ramos, “Chiral unitary approach to the K^- deuteron scattering length”, *Nucl. Phys. A* **690** (2001) 494–508, arXiv:nucl-th/0010054.
- [55] J. Arvieux, “Phase-shift analysis of elastic proton-deuteron scattering cross sections and ^3He excited states”, *Nucl. Phys. A* **221** (1974) 253–268.
- [56] W. T. H. Van Oers *et al.*, “Phase-shift analysis of elastic nucleon-deuteron scattering”, *Nucl. Phys. A* **92** (1967) 561–583.
- [57] E. Huttel *et al.*, “Phase-shift analysis of p–d elastic scattering below break-up threshold”, *Nucl. Phys. A* **406** (1983) 443–455.
- [58] A. Kievsky *et al.*, “The Three nucleon system near the N–d threshold”, *Phys. Lett. B* **406** (1997) 292–296, arXiv:nucl-th/9706077.
- [59] T. C. Black *et al.*, “Determination of proton-deuteron scattering lengths”, *Phys. Lett. B* **471** (1999) 103–107.
- [60] S. Pratt, “Pion interferometry of quark-gluon plasma”, *Phys. Rev. D* **33** (1986) 1314–1327.
- [61] M. Lisa *et al.*, “Femtoscopia in relativistic heavy-ion collisions”, *Ann. Rev. Nucl. Part. Sci.* **55** (2005) 357–402.

- [62] R. Lednicky and V. L. Lyuboshits, “Final state interaction effect on pairing correlations between particles with small relative momenta”, *Yad. Fiz.* **35** (1981) 1316–1330.
- [63] R. Lednicky, “Finite-size effects on two-particle production in continuous and discrete spectrum”, *Phys. Part. Nucl.* **40** (2009) 307–352, arXiv:nuc1-th/0501065.
- [64] D. Mihaylov, V. Mantovani Sarti, O. Arnold, L. Fabbietti, B. Hohlweger, and A. Mathis, “A femtoscopic Correlation Analysis Tool using the Schrödinger equation (CATS)”, *Eur. Phys. J. C* **78** (2018) 394.
- [65] ALICE Collaboration, S. Acharya *et al.*, “Exploring the $NA-N\Sigma$ coupled system with high precision correlation techniques at the LHC”, *Phys. Lett. B* **833** (2022) 137272, arXiv:104.04427 [nucl-ex].
- [66] S. Mrówczyński, “Production of light nuclei at colliders – coalescence vs. thermal model”, *Eur. Phys. J. ST* **229** (2020) 3559–3583, arXiv:2004.07029 [nucl-th].
- [67] S. Mrówczyński and P. Słoń, “Deuteron–deuteron correlation function in nucleus-nucleus collisions”, *Phys. Rev. C* **104** (2021) 024909, arXiv:2103.15761 [nucl-th].
- [68] M. Viviani, S. König, A. Kievsky, L. E. Marcucci, B. Singh, and O. Vázquez Doce, “Role of three-body dynamics in nucleon-deuteron correlation functions”, arXiv:2306.02478 [nucl-th].
- [69] H.-W. Hammer, S. König, and U. van Kolck, “Nuclear effective field theory: status and perspectives”, *Rev. Mod. Phys.* **92** (2020) 025004.
- [70] ALICE Collaboration, “ALICE upgrades during the LHC Long Shutdown 2”, arXiv:2302.01238 [physics.ins-det].
- [71] Z. Citron *et al.*, “Report from Working Group 5: Future physics opportunities for high-density QCD at the LHC with heavy-ion and proton beams”, *CERN Yellow Rep. Monogr.* **7** (2019) 1159–1410.
- [72] ALICE Collaboration, K. Aamodt *et al.*, “The ALICE experiment at the CERN LHC”, *JINST* **3** (2008) S08002.
- [73] ALICE Collaboration, B. Abelev *et al.*, “Performance of the ALICE Experiment at the CERN LHC”, *Int. J. Mod. Phys. A* **29** (2014) 1430044.
- [74] ALICE Collaboration, S. Acharya *et al.*, “Investigation of the $p-\Sigma^0$ interaction via femtoscopy in pp collisions”, *Phys. Lett. B* **805** (2020) 135419, arXiv:1910.14407 [nucl-ex].
- [75] ALICE Collaboration, E. Abbas *et al.*, “Performance of the ALICE VZERO system”, *JINST* **8** (2013) P10016.
- [76] ALICE Collaboration, K. Aamodt *et al.*, “Alignment of the ALICE Inner Tracking System with cosmic-ray tracks”, *JINST* **5** (2010) P03003.
- [77] J. Alme *et al.*, “The ALICE TPC, a large 3-dimensional tracking device with fast readout for ultra-high multiplicity events”, *Nucl. Instrum. Meth. A* **622** (2010) 316–367.
- [78] A. Akindinov *et al.*, “Performance of the ALICE Time-Of-Flight detector at the LHC”, *Eur. Phys. J. Plus* **128** (2013) 44.
- [79] ALICE Collaboration, S. Acharya *et al.*, “Study of the $p-p-K^+$ and $p-p-K^-$ dynamics using the femtoscopy technique”, arXiv:2303.13448 [nucl-ex].

[80] V. Vovchenko and H. Stoecker, “Thermal-fist: A package for heavy-ion collisions and hadronic equation of state”, *Comput. Phys. Commun.* **244** (2019) 295–310.

Methods

Event selection

A data sample of inelastic pp collisions at $\sqrt{s} = 13$ TeV was recorded with ALICE [72, 73] at the LHC. General details on the event selection, pile-up rejection, and the primary vertex reconstruction can be found in [74]. A trigger that requires the total signal amplitude measured in the V0 detector [75] to exceed a certain threshold was employed to select high-multiplicity (HM) events. The V0 detector comprises two plastic scintillator arrays placed on both sides of the interaction point at pseudorapidities $2.8 < \eta < 5.1$ and $-3.7 < \eta < -1.7$. The pseudorapidity is defined as $\eta = -\ln \left[\tan \left(\frac{\theta}{2} \right) \right]$, where θ is the polar angle of the particle with respect to the proton beam axis.

At $\sqrt{s} = 13$ TeV, the average number of charged particles produced in HM events in the range $|\eta| < 0.5$ is 30. This η range corresponds to the region within 26 degrees of the transverse plane perpendicular to the beam axis. The HM events constitute only 0.17% of the pp collisions that produce at least one charged particle in the pseudorapidity range $|\eta| < 1.0$. A total of 1×10^9 HM events were analyzed. Additional details on the HM event selection can be found in [74].

Particle Tracking and Identification

For the identification and momentum measurement of charged particles, the Inner Tracking System (ITS) [76], Time Projection Chamber (TPC) [77], and Time-Of-Flight (TOF) [78] detectors of ALICE are employed. All three detectors are located inside a uniform magnetic field generated by the L3 solenoid (0.5 T), leading to a bending of the trajectories of charged particles. The measurement of the curvature is used to reconstruct the particle momenta. Typical transverse momentum (p_T) resolutions for kaons, protons, and deuterons vary from about 2% for tracks with $p_T = 10$ GeV/c to below 1% for $p_T < 1$ GeV/c. The particle identity is determined by the energy lost per unit of track length inside the TPC detector and by the particle velocity measured in the TOF detector. For additional experimental details, see [73]. Basic details on the selection criteria of the proton, kaon, and deuteron tracks used in this work can be found in [79].

Kaons are identified via the measurement of the specific energy loss in TPC within a momentum range $p \in [0.2, 2.0]$ GeV/c. This information is combined with the time of flight measurement for momentum $p > 0.4$ GeV/c. In the kaon sample, the contamination from electrons produced via photon conversion in the detector material is removed by excluding kaon candidates in the momentum range $0.5 < p < 0.65$ GeV/c. The selected candidates that simultaneously fulfill the selection criteria of the pion (using TPC and TOF information) or proton (using TPC information) are also excluded from the sample.

Protons are selected within a transverse momentum range of $0.5 < p_T < 4.05$ GeV/c. They are identified by requiring TPC information for candidate tracks with momentum $p < 0.75$ GeV/c, while TPC and TOF information are both required for candidates with $p > 0.75$ GeV/c. The identification of deuterons is performed with the TPC in the momentum range $0.4 < p < 1.4$ GeV/c. For the analysis of $K^+ - d$ pairs, the deuteron acceptance is extended by using TOF identification in the region $1.4 < p < 2.3$ GeV/c.

The selection of kaons, protons and deuterons constitute the main source of systematic uncertainties associated to the measured correlation function. All particle selection criteria are varied with respect to their default values. In order to account for the effect of possible correlations, the analysis of $K^+ - d$ ($p - d$) pairs is repeated 40 (44) times using random combinations of such selection criteria. The associated systematic uncertainty of the measured correlation function for each k^* point is given by the root mean

square of all 40 (44) resulting correlation functions. The total systematic uncertainties are maximal at low k^* , reaching a value of 3% and 7% for K^+-d and $p-d$, correspondingly.

Characterization of the source of particles

The distribution $S(r^*)$ of the distance r^* at which particles are emitted, is described by a Gaussian function whose width characterizes the source size. In [40], the baryon–baryon source sizes are determined as a function of the transverse mass of the baryon–baryon pair, $m_T = (k_T^2 + m^2)^{1/2}$, where m is the average mass and $k_T = |\mathbf{p}_{T,1} + \mathbf{p}_{T,2}|/2$ is the transverse momentum of the pair. For $p-d$ and K^+-d pairs, it is assumed that the common source for all baryons still holds for any hadron–hadron pair [40]. The measured $\langle m_T \rangle$ for $p-d$ and K^+-d pairs are 1.64 GeV/ c and 1.50 GeV/ c , respectively, implying source sizes of $r_{\text{core}}^{K^+-d} = 1.04 \pm 0.04$ fm and $r_{\text{core}}^{p-d} = 0.99 \pm 0.05$ fm, where r_{core} denotes the width of the Gaussian distribution defining the source before taking into account the effect produced by short-lived resonances.

In pp collisions at $\sqrt{s} = 13$ TeV, about 2/3 of the protons and 1/3 of the kaons originate from the decay of short-lived resonances with a lifetime ($c\tau$) of a few fm. Table 2 shows the major relative contributions to the proton and kaon samples by several resonances, according to statistical hadronization [80]. The effect of such resonances on the source size is evaluated by folding the Gaussian source with an exponential distribution containing the resonance decay constant, following [40]. The resulting source distribution for $p-d$ can be parameterized with an effective Gaussian source radius equal to $r_{\text{eff}}^{p-d} = 1.08 \pm 0.06$ fm. For K^+-d pairs, the resulting source distribution is described using a sum of two Gaussian functions with radii 1.10 ± 0.04 fm and $2.14_{-0.07}^{+0.03}$ fm with weights of 0.76 and 0.24, respectively. The effective source size quoted in the text $r_{\text{eff}}^{K^+-d} = 1.35_{-0.05}^{+0.04}$ fm results from the weighted sum of the two Gaussians. Note that a description with a single Gaussian (1G) for the K^+-d source distribution, including the effects of resonances is not satisfactory, but it is nevertheless illustrative to compare the resulting radius of $r_{\text{eff}1G}^{K^+-d} = 1.22 \pm 0.04$ fm with the $p-d$ radius $r_{\text{eff}}^{p-d} = 1.08 \pm 0.06$ fm.

In the case of the three-body calculation for the $p-d$ system, the formalism requires as input the two-particle source size for each pairwise source of the $p-(pn)$ system. For nucleon pairs an average core source size of $r_{\text{core}}^{\text{NN}} = 1.35 \pm 0.14$ fm has been estimated using the measured $\langle m_T \rangle$ for $p-d$ and the measured $\langle p_T \rangle$ of deuteron and protons below $k^* < 400$ MeV/ c . The source size $r_{\text{core}}^{\text{NN}}$ is enhanced by the strongly decaying resonances that feed to protons and neutrons. Similar to the case of $p-d$ and K^+-d pairs this effect in the source size is taken into account by folding the Gaussian source with an exponential distribution. The resulting source distribution for NN pairs can be characterized by an effective Gaussian source radius equal to $r_{\text{eff}}^{\text{NN}} = 1.43_{-0.16}^{+0.16}$ fm. This source size is an average of distances between the $p-p$ and $p-n$ pairs that form the $p-d$ system.

Corrections of the Correlation Function

The experimental correlation function, defined as $C(k^*) = \xi(k^*) \otimes \frac{N_{\text{same}}(k^*)}{N_{\text{mixed}}(k^*)}$, is corrected, via $\xi(k^*)$, for normalization and the unfolding of momentum resolution effects. A normalization factor \mathcal{N} is used to correct for the different yields in same- and mixed-event distributions. The value of the normalization factor is chosen such that the mean value of the correlation function is equal to unity. It is obtained by dividing the integral of the $N_{\text{same}}(k^*)$ and $N_{\text{mixed}}(k^*)$ in a region where the effect of final-state interactions is negligible (for $p-d$: $200 < k^* < 500$ MeV/ c and in the case of K^+-d : $300 < k^* < 600$ MeV/ c).

The shape of the measured correlation function is affected by the finite resolution in the determination of the momentum of particles. The measured same- and mixed-event distributions are unfolded for the momentum smearing using MC simulations. The correction for the measured correlation function due to the momentum resolution effect with the MC event generator is found to be at most 3% for $p-d$ and 9% for K^+-d at low k^* . Moreover, the resolution effects due to the merging of trajectories which cross the

Table 2: Fractions of protons and kaons feeding from the strongly-decaying short-lived decays of resonances. The contribution of kaons from the $\phi(1020)$ decays are considered as feed-down to the correlation functions.

protons			kaons		
resonances	$c\tau(\text{fm})$	fractions(%)	resonances	$c\tau(\text{fm})$	fractions(%)
Δ^{++}	1.64	21.87	$K^*(892)^0$	3.89	21
Δ^+	1.64	14.60	$K^*(892)^+$	3.88	11
Δ^0	1.64	7.20	$a_0(980)^+$	2.63	1
$N(1440)^0$	0.56	0.91	$K_2^*(1430)^0$	1.81	1
$N(1520)^0$	1.64	1.75	$K_1^*(1270)^0$	2.19	1
$N(1680)^0$	1.52	1.15	$\phi(1020)$	46.32	(6)
$N(1535)^+$	1.31	1.02	–	–	–
$N(1440)^+$	0.56	0.91	–	–	–

detector at a distance comparable with the spatial resolution of the detector (ITS or TPC) were evaluated and found to be negligible.

While the measured p–d and K^+ –d correlation functions are dominated by the interaction between p–d and K^+ –d pairs consisting of primary particles produced in the collision, they are also influenced by the effects caused by the misidentification of particles and by the contribution of secondary particles produced in weak decays. Due to the large decay times of weakly decaying particles, the final-state interaction between their decay products and the primary particle of interest is absent, thus leading to either a flat contribution or a residual signature of the interaction with the parent hadron. The contributions to $C(k^*)$ from the genuine correlation of primary particles, the misidentified hadrons, and the secondary particles are quantified by the so-called λ parameters, which are computed from the purity and the primary fraction of each particle species as described in [33]. The λ parameters for the genuine correlation function of p–d and K^+ –d are listed in Table 3. All the residual correlations not stemming from genuine primary pairs in the p–d and K^+ –d correlation functions are assumed to be equal to unity regardless of the values of k^* and the theoretical correlation functions shown in Figs. 1 and 2 are corrected using the corresponding λ parameters.

Table 3: λ parameters of the genuine particle pairs for p–d and K^+ –d.

λ parameter	value
λ_{pd}	79.7%
$\lambda_{p\bar{d}}$	84.1%
λ_{K^+d}	90.1%
$\lambda_{K^-\bar{d}}$	94.1%

The uncertainties on the determination of the residual contributions and the source size are propagated to the theoretical correlation functions and contribute, together with the intrinsic theoretical uncertainties of each model, to the width of the bands shown in Fig. 1 and Fig. 2.

In addition to the residual correlation, the theoretical correlation function is also corrected for the rising tail effect of the experimental correlation in the region where the final-state interaction is negligible and that can be originated from effects such as energy conservation. A multiplicative cubic baseline $BL(k^*) = a + bk^{*2} + ck^{*3}$ is used to describe the data at large k^* . For K^+ –d correlations, the baseline is pre-fitted in the region of $300 < k^* < 1800$ MeV/c. In the case of the p–d correlation function, the parameters a , b and c are obtained from a fit to the data in the region $0 < k^* < 700$ MeV/c including the theoretical correlation function and the multiplicative baseline. The baseline is represented by the gray bands in Figs. 1 and 2.

The Lednický-Lyuboshitz Model

The final-state interaction for two charged point-like particles has been modeled in [63]. The definition of the relative s -wave function for a system of two charged point-like distinguishable particles is given as

$$\psi(\vec{k}^*, \vec{r}^*) = e^{i\delta_c} \sqrt{A_C(\eta)} \left[e^{-i\vec{k}^* \cdot \vec{r}^*} F(-i\eta, 1, i\xi) + f_C(k^*) \frac{\tilde{G}(\rho, \eta)}{r^*} \right], \quad (1)$$

where $\eta = (k^* a_C)^{-1}$, a_C is the Bohr radius including the sign of the interaction between the pair of particles, $\xi = \rho(1 + \cos(\theta^*))$, and $\rho = k^* r^*$. Where θ^* is the angle between \vec{k}^* and \vec{r}^* . The term $A_C(\eta) = 2\pi\eta [\exp(2\pi\eta) - 1]^{-1}$ is a Coulomb-barrier penetration factor, also known as Gamow factor. The Coulomb interaction (asymptotic form) in the wave function is described by the term $e^{-i\vec{k}^* \cdot \vec{r}^*} F(\alpha, 1, z)$ together with $\tilde{G}(\rho, \eta)$, where $F(\alpha, 1, z) = 1 + \frac{\alpha z}{12} + \frac{\alpha(\alpha+1)z^2}{12^2} + \dots$ is a confluent hypergeometric function and $\tilde{G}(\rho, \eta) = \sqrt{A_C}(G_0 + iF_0)$ is a combination of the regular (F_0) and singular (G_0) s -wave Coulomb functions. The strong nuclear interaction is computed using the Coulomb-corrected scattering amplitude f_C defined as

$$f_C(k^*) = \left[\frac{1}{-a_0} + \frac{d_0 k^{*2}}{2} - i k^* A_C(k^*) - \frac{2}{a_C} h(k^*) \right]^{-1}. \quad (2)$$

The function $h(k^*)$ is written as $h(k^*) = \frac{1}{(k^* a_C)^2} \sum_{n=1}^{\infty} [n(n^2 + (k^* a_C)^{-2})]^{-1} - \gamma + \ln |k^* a_C|$, where the constant $\gamma = 0.5772$ is the Euler constant.

Three-body formalism for the p–d correlation function

In order to account for the internal structure of the deuteron, a calculation of the proton–deuteron correlation function that includes a microscopic p–d wave function $\Psi_{m_2, m_1}(\mathbf{x}, \mathbf{y})$ has been carried out. This wave function accounts for all the relevant two- and three-body interactions at work in the p–(pn) system for the short and asymptotic ranges. It accurately describes the three-body dynamics [16–18] since it is tuned on p–d scattering observables. The variables \mathbf{x} and \mathbf{y} are the Jacobi vectors of the system, and they asymptotically denote the distance of the p–n system within the deuteron and the p–d distance, respectively. The indices m_2 and m_1 are quantum numbers of the spin operators for the deuteron and the proton when they are very well apart. The three-body correlation is calculated using the formalism discussed in [66, 67]. More details about the employed wave functions and the computation of the p–d correlation function can be found in [68]. In general, the formalism is based on the following expressions

$$C_{pd}(k) = \frac{1}{A_d} \frac{1}{6} \sum_{m_2, m_1} \int d^3 r_1 d^3 r_2 d^3 r_3 S_1(r_1) S_1(r_2) S_1(r_3) |\Psi_{m_2, m_1}|^2, \quad (3)$$

$$A_d = \frac{1}{3} \sum_{m_2} \int d^3 r_1 d^3 r_2 S_1(r_1) S_1(r_2) |\phi_{m_2}|^2, \quad (4)$$

$$S_1(r) = \frac{1}{(2\pi R_M^2)^{\frac{3}{2}}} e^{-r^2/2R_M^2}, \quad (5)$$




















where ϕ_{m_2} is the deuteron wave function and $S_1(r)$ represents the single particle source term of radius R_M , while the factor 6 in the denominator of Eq. 3 takes into account the possible spin configurations. The quantity A_d can be related to the probability of deuteron formation in the reaction. Note that in this calculation, the accurate p–d wave function is different from the approximated form employed in [66, 67]. By considering a suitable choice of coordinates, one can demonstrate [19] that the parameter R_M corresponds to the effective radius for the two-nucleon system. For the p–d system, R_M has been estimated considering the measured $\langle m_T \rangle$ of the p–d pairs and the average transverse momentum $\langle p_T \rangle$ of the deuterons and protons used for the correlation. The value $R_M = r_{\text{eff}}^{\text{NN}} = 1.43_{-0.16}^{+0.16}$ fm has been obtained and used in the calculation.

A The ALICE Collaboration

S. Acharya ¹²⁹, D. Adamová ⁸⁹, G. Aglieri Rinella ³⁵, M. Agnello ³², N. Agrawal ⁵³, Z. Ahammed ¹³⁷, S. Ahmad ¹⁶, S.U. Ahn ⁷⁴, I. Ahuja ⁴⁰, A. Akhmedov ¹⁴⁶, M. Al-Turany ¹⁰⁰, D. Aleksandrov ¹⁴⁶, B. Alessandro ⁵⁹, H.M. Alfanda ⁶, R. Alfaro Molina ⁷⁰, B. Ali ¹⁶, A. Alici ²⁸, N. Alizadehvandchali ¹¹⁸, A. Alkin ³⁵, J. Alme ²², G. Alocco ⁵⁴, T. Alt ⁶⁷, A.R. Altamura ⁵², I. Altsybeev ⁹⁸, M.N. Anaam ⁶, C. Andrei ⁴⁸, N. Andreou ¹¹⁷, A. Andronic ¹⁴⁰, V. Anguelov ⁹⁷, F. Antinori ⁵⁶, P. Antonioli ⁵³, N. Apadula ⁷⁷, L. Aphecetche ¹⁰⁶, H. Appelshäuser ⁶⁷, C. Arata ⁷⁶, S. Arcelli ²⁸, M. Aresti ²⁴, R. Arnaldi ⁵⁹, J.G.M.C.A. Arneiro ¹¹³, I.C. Arsene ²¹, M. Arslandok ¹⁴², A. Augustinus ³⁵, R. Averbeck ¹⁰⁰, M.D. Azmi ¹⁶, H. Baba ¹²⁶, A. Badalà ⁵⁵, J. Bae ¹⁰⁷, Y.W. Baek ⁴³, X. Bai ¹²², R. Bailhache ⁶⁷, Y. Bailung ⁵⁰, A. Balbino ³², A. Baldisseri ¹³², B. Balis ², D. Banerjee ⁴, Z. Banoo ⁹⁴, R. Barbera ²⁹, F. Barile ³⁴, L. Barioglio ⁹⁸, M. Barlou ⁸¹, B. Barman ⁴⁴, G.G. Barnaföldi ¹⁴¹, L.S. Barnby ⁸⁸, V. Barret ¹²⁹, L. Barreto ¹¹³, C. Bartels ¹²¹, K. Barth ³⁵, E. Bartsch ⁶⁷, N. Bastid ¹²⁹, S. Basu ⁷⁸, G. Batigne ¹⁰⁶, D. Battistini ⁹⁸, B. Batyunya ¹⁴⁷, D. Bauri ⁴⁹, J.L. Bazo Alba ¹⁰⁴, I.G. Bearden ⁸⁶, C. Beattie ¹⁴², P. Becht ¹⁰⁰, D. Behera ⁵⁰, I. Belikov ¹³¹, A.D.C. Bell Hechavarria ¹⁴⁰, F. Bellini ²⁸, R. Bellwied ¹¹⁸, S. Belokurova ¹⁴⁶, Y.A.V. Beltran ⁴⁷, G. Bencedi ¹⁴¹, S. Beole ²⁷, Y. Berdnikov ¹⁴⁶, A. Berdnikova ⁹⁷, L. Bergmann ⁹⁷, M.G. Besoiu ⁶⁶, L. Betev ³⁵, P.P. Bhaduri ¹³⁷, A. Bhasin ⁹⁴, M.A. Bhat ⁴, B. Bhattacharjee ⁴⁴, L. Bianchi ²⁷, N. Bianchi ⁵¹, J. Bielčik ³⁸, J. Bielčíková ⁸⁹, J. Biernat ¹¹⁰, A.P. Bigot ¹³¹, A. Bilandzic ⁹⁸, G. Biro ¹⁴¹, S. Biswas ⁴, N. Bize ¹⁰⁶, J.T. Blair ¹¹¹, D. Blau ¹⁴⁶, M.B. Blidaru ¹⁰⁰, N. Bluhme ⁴¹, C. Blume ⁶⁷, G. Boca ^{23,57}, F. Bock ⁹⁰, T. Bodova ²², A. Bogdanov ¹⁴⁶, S. Boi ²⁴, J. Bok ⁶¹, L. Boldizsár ¹⁴¹, M. Bombara ⁴⁰, P.M. Bond ³⁵, G. Bonomi ^{136,57}, H. Borel ¹³², A. Borissov ¹⁴⁶, A.G. Borquez Carcamo ⁹⁷, H. Bossi ¹⁴², E. Botta ²⁷, Y.E.M. Bouziani ⁶⁷, L. Bratrud ⁶⁷, P. Braun-Munzinger ¹⁰⁰, M. Bregant ¹¹³, M. Broz ³⁸, G.E. Bruno ^{99,34}, M.D. Buckland ²⁶, D. Budnikov ¹⁴⁶, H. Buesching ⁶⁷, S. Bufalino ³², P. Buhler ¹⁰⁵, N. Burmasov ¹⁴⁶, Z. Buthelezi ^{71,125}, A. Bylinkin ²², S.A. Bysiak ¹¹⁰, M. Cai ⁶, H. Caines ¹⁴², A. Caliva ³¹, E. Calvo Villar ¹⁰⁴, J.M.M. Camacho ¹¹², P. Camerini ²⁶, F.D.M. Canedo ¹¹³, M. Carabas ¹²⁸, A.A. Carballo ³⁵, F. Carnesecchi ³⁵, R. Caron ¹³⁰, L.A.D. Carvalho ¹¹³, J. Castillo Castellanos ¹³², F. Catalano ^{35,27}, C. Ceballos Sanchez ¹⁴⁷, I. Chakaberia ⁷⁷, P. Chakraborty ⁴⁹, S. Chandra ¹³⁷, S. Chapeland ³⁵, M. Chartier ¹²¹, S. Chattopadhyay ¹³⁷, S. Chattopadhyay ¹⁰², T.G. Chavez ⁴⁷, T. Cheng ^{100,6}, C. Cheshkov ¹³⁰, B. Cheynis ¹³⁰, V. Chibante Barroso ³⁵, D.D. Chinellato ¹¹⁴, E.S. Chizzali ^{1,98}, J. Cho ⁶¹, S. Cho ⁶¹, P. Chochula ³⁵, D. Choudhury ⁴⁴, P. Christakoglou ⁸⁷, C.H. Christensen ⁸⁶, P. Christiansen ⁷⁸, T. Chujo ¹²⁷, M. Ciacco ³², C. Cicalo ⁵⁴, F. Cindolo ⁵³, M.R. Ciupek ¹⁰⁰, G. Clai ^{II,53}, F. Colamaria ⁵², J.S. Colburn ¹⁰³, D. Colella ^{99,34}, M. Colocci ²⁸, M. Concas ^{III,35}, G. Conesa Balbastre ⁷⁶, Z. Conesa del Valle ¹³³, G. Contin ²⁶, J.G. Contreras ³⁸, M.L. Coquet ¹³², P. Cortese ^{135,59}, M.R. Cosentino ¹¹⁵, F. Costa ³⁵, S. Costanza ^{23,57}, C. Cot ¹³³, J. Crkovská ⁹⁷, P. Crochet ¹²⁹, R. Cruz-Torres ⁷⁷, P. Cui ⁶, A. Dainese ⁵⁶, M.C. Danisch ⁹⁷, A. Danu ⁶⁶, P. Das ⁸³, P. Das ⁴, S. Das ⁴, A.R. Dash ¹⁴⁰, S. Dash ⁴⁹, R.M.H. David ⁴⁷, A. De Caro ³¹, G. de Cataldo ⁵², J. de Cuveland ⁴¹, A. De Falco ²⁴, D. De Gruttola ³¹, N. De Marco ⁵⁹, C. De Martin ²⁶, S. De Pasquale ³¹, R. Deb ¹³⁶, R. Del Grande ⁹⁸, L. Dello Stritto ³¹, W. Deng ⁶, P. Dhankher ¹⁹, D. Di Bari ³⁴, A. Di Mauro ³⁵, B. Diab ¹³², R.A. Diaz ^{147,7}, T. Dietel ¹¹⁶, Y. Ding ⁶, J. Ditzel ⁶⁷, R. Divià ³⁵, D.U. Dixit ¹⁹, Ø. Djuvsland ²², U. Dmitrieva ¹⁴⁶, A. Dobrin ⁶⁶, B. Dönigus ⁶⁷, J.M. Dubinski ¹³⁸, A. Dubla ¹⁰⁰, S. Dudi ⁹³, P. Dupieux ¹²⁹, M. Durkac ¹⁰⁹, N. Dzalaiova ¹³, T.M. Eder ¹⁴⁰, R.J. Ehlers ⁷⁷, F. Eisenhut ⁶⁷, R. Ejima ⁹⁵, D. Elia ⁵², B. Erazmus ¹⁰⁶, F. Ercolessi ²⁸, B. Espagnon ¹³³, G. Eulisse ³⁵, D. Evans ¹⁰³, S. Evdokimov ¹⁴⁶, L. Fabbietti ⁹⁸, M. Faggin ³⁰, J. Faivre ⁷⁶, F. Fan ⁶, W. Fan ⁷⁷, A. Fantoni ⁵¹, M. Fasel ⁹⁰, P. Fecchio ³², A. Feliciello ⁵⁹, G. Feofilov ¹⁴⁶, A. Fernández Téllez ⁴⁷, L. Ferrandi ¹¹³, M.B. Ferrer ³⁵, A. Ferrero ¹³², C. Ferrero ⁵⁹, A. Ferretti ²⁷, V.J.G. Feuillard ⁹⁷, V. Filova ³⁸, D. Finogeev ¹⁴⁶, F.M. Fionda ⁵⁴, F. Flor ¹¹⁸, A.N. Flores ¹¹¹, S. Foertsch ⁷¹, I. Fokin ⁹⁷, S. Fokin ¹⁴⁶, E. Fragiaco ⁶⁰, E. Frajna ¹⁴¹, U. Fuchs ³⁵, N. Funicello ³¹, C. Furget ⁷⁶, A. Furs ¹⁴⁶, T. Fusayasu ¹⁰¹, J.J. Gaardhøje ⁸⁶, M. Gagliardi ²⁷, A.M. Gago ¹⁰⁴, T. Gahlaut ⁴⁹, C.D. Galvan ¹¹², D.R. Gangadharan ¹¹⁸, P. Ganoti ⁸¹, C. Garabatos ¹⁰⁰, A.T. Garcia ¹³³, J.R.A. Garcia ⁴⁷, E. Garcia-Solis ⁹, C. Gargiulo ³⁵, P. Gasik ¹⁰⁰, A. Gautam ¹²⁰, M.B. Gay Ducati ⁶⁹, M. Germain ¹⁰⁶, A. Ghimouz ¹²⁷, C. Ghosh ¹³⁷, M. Giacalone ⁵³, G. Gioachin ³², P. Giubellino ^{100,59}, P. Giubilato ³⁰, A.M.C. Glaenger ¹³², P. Glässel ⁹⁷, E. Glimos ¹²⁴, D.J.Q. Goh ⁷⁹, V. Gonzalez ¹³⁹, M. Gorgon ², K. Goswami ⁵⁰, S. Gotovac ³⁶, V. Grabski ⁷⁰, L.K. Graczykowski ¹³⁸, E. Grecka ⁸⁹, A. Grelli ⁶², C. Grigoras ³⁵, V. Grigoriev ¹⁴⁶, S. Grigoryan ^{147,1}, F. Grosa ³⁵, J.F. Grosse-Oetringhaus ³⁵, R. Grosso ¹⁰⁰, D. Grund ³⁸, N.A. Grunwald ⁹⁷, G.G. Guardiani ¹¹⁴, R. Guernane ⁷⁶, M. Guilbaud ¹⁰⁶, K. Gulbrandsen ⁸⁶, T. Gündem ⁶⁷, T. Gunji ¹²⁶,

W. Guo⁶, A. Gupta⁹⁴, R. Gupta⁹⁴, R. Gupta⁵⁰, S.P. Guzman⁴⁷, K. Gwizdziel¹³⁸, L. Gyulai¹⁴¹,
 C. Hadjidakis¹³³, F.U. Haider⁹⁴, S. Haidlova³⁸, H. Hamagaki⁷⁹, A. Hamdi⁷⁷, Y. Han¹⁴³,
 B.G. Hanley¹³⁹, R. Hannigan¹¹¹, J. Hansen⁷⁸, M.R. Haque¹³⁸, J.W. Harris¹⁴², A. Harton⁹,
 H. Hassan¹¹⁹, D. Hatzifotiadou⁵³, P. Hauer⁴⁵, L.B. Havener¹⁴², S.T. Heckel⁹⁸, E. Hellbär¹⁰⁰,
 H. Helstrup³⁷, M. Hemmer⁶⁷, T. Herman³⁸, G. Herrera Corral⁸, F. Herrmann¹⁴⁰, S. Herrmann¹³⁰,
 K.F. Hetland³⁷, B. Heybeck⁶⁷, H. Hillemanns³⁵, B. Hippolyte¹³¹, F.W. Hoffmann⁷³, B. Hofman⁶²,
 G.H. Hong¹⁴³, M. Horst⁹⁸, A. Horzyk², Y. Hou⁶, P. Hristov³⁵, C. Hughes¹²⁴, P. Huhn⁶⁷,
 L.M. Huhta¹¹⁹, T.J. Humanic⁹¹, A. Hutson¹¹⁸, D. Hutter⁴¹, R. Ilkaev¹⁴⁶, H. Ilyas¹⁴, M. Inaba¹²⁷,
 G.M. Innocenti³⁵, M. Ippolitov¹⁴⁶, A. Isakov^{87,89}, T. Isidori¹²⁰, M.S. Islam¹⁰², M. Ivanov¹⁰⁰,
 M. Ivanov¹³, V. Ivanov¹⁴⁶, K.E. Iversen⁷⁸, M. Jablonski², B. Jacak⁷⁷, N. Jacazio²⁸, P.M. Jacobs⁷⁷,
 S. Jadlovská¹⁰⁹, J. Jadlovsky¹⁰⁹, S. Jaelani⁸⁵, C. Jahnke¹¹⁴, M.J. Jakubowska¹³⁸, M.A. Janik¹³⁸,
 T. Janson⁷³, S. Ji¹⁷, S. Jia¹⁰, A.A.P. Jimenez⁶⁸, F. Jonas⁹⁰, D.M. Jones¹²¹, J.M. Jowett^{35,100},
 J. Jung⁶⁷, M. Jung⁶⁷, A. Junique³⁵, A. Jusko¹⁰³, M.J. Kabus^{35,138}, J. Kaewjai¹⁰⁸, P. Kalinak⁶³,
 A.S. Kalteyer¹⁰⁰, A. Kalweit³⁵, V. Kaplin¹⁴⁶, A. Karasu Uysal⁷⁵, D. Karatovic⁹²,
 O. Karavichev¹⁴⁶, T. Karavicheva¹⁴⁶, P. Karczmarczyk¹³⁸, E. Karpechev¹⁴⁶, U. Kebschull⁷³,
 R. Keidel¹⁴⁵, D.L.D. Keijdener⁶², M. Keil³⁵, B. Ketzer⁴⁵, S.S. Khade⁵⁰, A.M. Khan^{122,6},
 S. Khan¹⁶, A. Khanzadeev¹⁴⁶, Y. Kharlov¹⁴⁶, A. Khatun¹²⁰, A. Khuntia³⁸, A. Kievsky⁵⁸,
 B. Kileng³⁷, B. Kim¹⁰⁷, C. Kim¹⁷, D.J. Kim¹¹⁹, E.J. Kim⁷², J. Kim¹⁴³, J.S. Kim⁴³, J. Kim⁶¹,
 J. Kim⁷², M. Kim¹⁹, S. Kim¹⁸, T. Kim¹⁴³, K. Kimura⁹⁵, S. Kirsch⁶⁷, I. Kisel⁴¹, S. Kiselev¹⁴⁶,
 A. Kisiel¹³⁸, J.P. Kitowski², J.L. Klay⁵, J. Klein³⁵, S. Klein⁷⁷, C. Klein-Bösing¹⁴⁰, M. Kleiner⁶⁷,
 T. Klemenz⁹⁸, A. Kluge³⁵, A.G. Knospe¹¹⁸, C. Kobdaj¹⁰⁸, T. Kollegger¹⁰⁰, A. Kondratyev¹⁴⁷,
 N. Kondratyeva¹⁴⁶, E. Kondratyuk¹⁴⁶, J. König⁶⁷, S. König²⁰, S.A. Königstorfer⁹⁸, P.J. Konopka³⁵,
 G. Kornakov¹³⁸, S.D. Koryciak², A. Kotliarov⁸⁹, V. Kovalenko¹⁴⁶, M. Kowalski¹¹⁰,
 V. Kozuharov³⁹, I. Králik⁶³, A. Kravčáková⁴⁰, L. Krcal^{35,41}, M. Krivda^{103,63}, F. Krizek⁸⁹,
 K. Krizkova Gajdosova³⁵, M. Kroesen⁹⁷, M. Krüger⁶⁷, D.M. Krupova³⁸, E. Kryshen¹⁴⁶,
 V. Kučera⁶¹, C. Kuhn¹³¹, P.G. Kuijer⁸⁷, T. Kumaoka¹²⁷, D. Kumar¹³⁷, L. Kumar⁹³, N. Kumar⁹³,
 S. Kumar³⁴, S. Kundu³⁵, P. Kurashvili⁸², A. Kurepin¹⁴⁶, A.B. Kurepin¹⁴⁶, A. Kuryakin¹⁴⁶,
 S. Kushpil⁸⁹, M.J. Kweon⁶¹, Y. Kwon¹⁴³, S.L. La Pointe⁴¹, P. La Rocca²⁹, A. Lakrathok¹⁰⁸,
 M. Lamanna³⁵, R. Langoy¹²³, P. Larionov³⁵, E. Laudi³⁵, L. Lautner^{35,98}, R. Lavicka¹⁰⁵,
 R. Lea^{136,57}, H. Lee¹⁰⁷, I. Legrand⁴⁸, G. Legras¹⁴⁰, J. Lehrbach⁴¹, T.M. Lelek², R.C. Lemmon⁸⁸,
 I. León Monzón¹¹², M.M. Lesch⁹⁸, E.D. Lesser¹⁹, P. Lévai¹⁴¹, X. Li¹⁰, J. Lien¹²³, R. Lietava¹⁰³,
 I. Likmeta¹¹⁸, B. Lim²⁷, S.H. Lim¹⁷, V. Lindenstruth⁴¹, A. Lindner⁴⁸, C. Lippmann¹⁰⁰, D.H. Liu⁶,
 J. Liu¹²¹, G.S.S. Liveraro¹¹⁴, I.M. Lofnes²², C. Loizides⁹⁰, S. Lokos¹¹⁰, J. Lomker⁶², P. Loncar³⁶,
 X. Lopez¹²⁹, E. López Torres⁷, P. Lu^{100,122}, F.V. Lugo⁷⁰, J.R. Luhder¹⁴⁰, M. Lunardon³⁰,
 G. Luparello⁶⁰, Y.G. Ma⁴², M. Mager³⁵, A. Maire¹³¹, M.V. Makariev³⁹, M. Malaev¹⁴⁶,
 G. Malfattore²⁸, N.M. Malik⁹⁴, Q.W. Malik²¹, S.K. Malik⁹⁴, L. Malinina^{VI,147}, D. Mallick^{133,83},
 N. Mallick⁵⁰, G. Mandaglio^{33,55}, S.K. Mandal⁸², V. Manko¹⁴⁶, F. Manso¹²⁹, V. Manzari⁵²,
 Y. Mao⁶, R.W. Marcjan², L.E. Marcucci²⁵, G.V. Margagliotti²⁶, A. Margotti⁵³, A. Marín¹⁰⁰,
 C. Markert¹¹¹, P. Martinengo³⁵, M.I. Martínez⁴⁷, G. Martínez García¹⁰⁶, M.P.P. Martins¹¹³,
 S. Masciocchi¹⁰⁰, M. Maserà²⁷, A. Masoni⁵⁴, L. Massacrier¹³³, O. Massen⁶², A. Mastroserio^{134,52},
 O. Matonoha⁷⁸, S. Mattiazzo³⁰, A. Matyja¹¹⁰, C. Mayer¹¹⁰, A.L. Mazuecos³⁵, F. Mazzaschi²⁷,
 M. Mazzilli³⁵, J.E. Mdhluli¹²⁵, Y. Melikyan⁴⁶, A. Menchaca-Rocha⁷⁰, J.E.M. Mendez⁶⁸,
 E. Meninno^{105,31}, A.S. Menon¹¹⁸, M. Meres¹³, S. Mhlanga^{116,71}, Y. Miake¹²⁷, L. Micheletti³⁵,
 D.L. Mihaylov⁹⁸, K. Mikhaylov^{147,146}, A.N. Mishra¹⁴¹, D. Miśkowiec¹⁰⁰, A. Modak⁴, B. Mohanty⁸³,
 M. Mohisin Khan^{IV,16}, M.A. Molander⁴⁶, S. Monira¹³⁸, C. Mordasini¹¹⁹, D.A. Moreira De
 Godoy¹⁴⁰, I. Morozov¹⁴⁶, A. Morsch³⁵, T. Mrnjavac³⁵, V. Muccifora⁵¹, S. Muhuri¹³⁷,
 J.D. Mulligan⁷⁷, A. Mulliri²⁴, M.G. Munhoz¹¹³, R.H. Munzer⁶⁷, H. Murakami¹²⁶, S. Murray¹¹⁶,
 L. Musa³⁵, J. Musinsky⁶³, J.W. Myrcha¹³⁸, B. Naik¹²⁵, A.I. Nambrath¹⁹, B.K. Nandi⁴⁹,
 R. Nania⁵³, E. Nappi⁵², A.F. Nassirpour¹⁸, A. Nath⁹⁷, C. Nattrass¹²⁴, M.N. Naydenov³⁹,
 A. Neagu²¹, A. Negru¹²⁸, L. Nellen⁶⁸, R. Nepeivoda⁷⁸, S. Nese²¹, G. Neskovic⁴¹, N. Nicassio⁵²,
 B.S. Nielsen⁸⁶, E.G. Nielsen⁸⁶, S. Nikolaev¹⁴⁶, S. Nikulin¹⁴⁶, V. Nikulin¹⁴⁶, F. Noferini⁵³,
 S. Noh¹², P. Nomokonov¹⁴⁷, J. Norman¹²¹, N. Novitzky⁹⁰, P. Nowakowski¹³⁸, A. Nyanin¹⁴⁶,
 J. Nystrand²², M. Ogino⁷⁹, S. Oh¹⁸, A. Ohlson⁷⁸, A. Ohnishi¹⁴⁴, V.A. Okorokov¹⁴⁶,
 J. Oleniacz¹³⁸, A.C. Oliveira Da Silva¹²⁴, A. Onnerstad¹¹⁹, C. Oppedisano⁵⁹, A. Ortiz Velasquez⁶⁸,
 J. Otwinowski¹¹⁰, M. Oya⁹⁵, K. Oyama⁷⁹, Y. Pachmayer⁹⁷, S. Padhan⁴⁹, D. Pagano^{136,57},
 G. Paić⁶⁸, A. Palasciano⁵², S. Panebianco¹³², H. Park¹²⁷, H. Park¹⁰⁷, J. Park⁶¹, J.E. Parkkila³⁵,

Y. Patley⁴⁹, R.N. Patra⁹⁴, B. Paul²⁴, H. Pei⁶, T. Peitzmann⁶², X. Peng¹¹, M. Pennisi²⁷,
 S. Perciballi²⁷, D. Peresunko¹⁴⁶, G.M. Perez⁷, Y. Pestov¹⁴⁶, V. Petrov¹⁴⁶, M. Petrovici⁴⁸,
 R.P. Pezzi^{106,69}, S. Piano⁶⁰, M. Pikna¹³, P. Pillot¹⁰⁶, O. Pinazza^{53,35}, L. Pinsky¹¹⁸, C. Pinto⁹⁸,
 S. Pisano⁵¹, M. Płoskoń⁷⁷, M. Planinic⁹², F. Pliquett⁶⁷, M.G. Poghosyan⁹⁰, B. Polichtchouk¹⁴⁶,
 S. Politano³², N. Poljak⁹², A. Pop⁴⁸, S. Porteboeuf-Houssais¹²⁹, V. Pozdniakov¹⁴⁷, I.Y. Pozos⁴⁷,
 K.K. Pradhan⁵⁰, S.K. Prasad⁴, S. Prasad⁵⁰, R. Preghenella⁵³, F. Prino⁵⁹, C.A. Pruneau¹³⁹,
 I. Pshenichnov¹⁴⁶, M. Puccio³⁵, S. Pucillo²⁷, Z. Pugelova¹⁰⁹, S. Qiu⁸⁷, L. Quaglia²⁷, S. Ragoni¹⁵,
 A. Rai¹⁴², A. Rakotozafindrabe¹³², L. Ramello^{135,59}, F. Rami¹³¹, S.A.R. Ramirez⁴⁷, T.A. Rancien⁷⁶,
 M. Rasa²⁹, S.S. Räsänen⁴⁶, R. Rath⁵³, M.P. Rauch²², I. Ravasenga⁸⁷, K.F. Read^{90,124},
 C. Reckziegel¹¹⁵, A.R. Redelbach⁴¹, K. Redlich^{5,82}, C.A. Reetz¹⁰⁰, A. Rehman²², F. Reidt³⁵,
 H.A. Reme-Ness³⁷, Z. Rescakova⁴⁰, K. Reygers⁹⁷, A. Riabov¹⁴⁶, V. Riabov¹⁴⁶, R. Ricci³¹,
 M. Richter²¹, A.A. Riedel⁹⁸, W. Riegler³⁵, A.G. Riffero²⁷, C. Ristea⁶⁶, M.V. Rodriguez³⁵,
 M. Rodríguez Cahuantzi⁴⁷, K. Røed²¹, R. Rogalev¹⁴⁶, E. Rogochaya¹⁴⁷, T.S. Rogoschinski⁶⁷,
 D. Rohr³⁵, D. Röhrich²², P.F. Rojas⁴⁷, S. Rojas Torres³⁸, P.S. Rokita¹³⁸, G. Romanenko²⁸,
 F. Ronchetti⁵¹, A. Rosano^{33,55}, E.D. Rosas⁶⁸, K. Roslon¹³⁸, A. Rossi⁵⁶, A. Roy⁵⁰, S. Roy⁴⁹,
 N. Rubini²⁸, D. Ruggiano¹³⁸, R. Rui²⁶, P.G. Russek², R. Russo⁸⁷, A. Rustamov⁸⁴,
 E. Ryabinkin¹⁴⁶, Y. Ryabov¹⁴⁶, A. Rybicki¹¹⁰, H. Rytkonen¹¹⁹, J. Ryu¹⁷, W. Rzesza¹³⁸,
 O.A.M. Saarimaki⁴⁶, S. Sadhu³⁴, S. Sadovsky¹⁴⁶, J. Saetre²², K. Šafařík³⁸, P. Saha⁴⁴, S.K. Saha⁴,
 S. Saha⁸³, B. Sahoo⁴⁹, B. Sahoo⁵⁰, R. Sahoo⁵⁰, S. Sahoo⁶⁴, D. Sahu⁵⁰, P.K. Sahu⁶⁴, J. Saini¹³⁷,
 K. Sajdakova⁴⁰, S. Sakai¹²⁷, M.P. Salvan¹⁰⁰, S. Sambyal⁹⁴, D. Samitz¹⁰⁵, I. Sanna^{35,98},
 T.B. Saramela¹¹³, P. Sarma⁴⁴, V. Sarritzu²⁴, V.M. Sarti⁹⁸, M.H.P. Sas¹⁴², S. Sawan⁸³, J. Schambach⁹⁰,
 H.S. Scheid⁶⁷, C. Schiaua⁴⁸, R. Schicker⁹⁷, A. Schmah¹⁰⁰, C. Schmidt¹⁰⁰, H.R. Schmidt⁹⁶,
 M.O. Schmidt³⁵, M. Schmidt⁹⁶, N.V. Schmidt⁹⁰, A.R. Schmier¹²⁴, R. Schotter¹³¹, A. Schröter⁴¹,
 J. Schukraft³⁵, K. Schweda¹⁰⁰, G. Scioli²⁸, E. Scomparin⁵⁹, J.E. Seger¹⁵, Y. Sekiguchi¹²⁶,
 D. Sekihata¹²⁶, M. Selina⁸⁷, I. Selyuzhenkov¹⁰⁰, S. Senyukov¹³¹, J.J. Seo^{97,61}, D. Serebryakov¹⁴⁶,
 L. Šerkšnytė⁹⁸, A. Sevcenco⁶⁶, T.J. Shaba⁷¹, A. Shabetai¹⁰⁶, R. Shahoyan³⁵, A. Shangaraev¹⁴⁶,
 A. Sharma⁹³, B. Sharma⁹⁴, D. Sharma⁴⁹, H. Sharma^{56,110}, M. Sharma⁹⁴, S. Sharma⁷⁹,
 S. Sharma⁹⁴, U. Sharma⁹⁴, A. Shatat¹³³, O. Sheibani¹¹⁸, K. Shigaki⁹⁵, M. Shimomura⁸⁰, J. Shin¹²,
 S. Shirinkin¹⁴⁶, Q. Shou⁴², Y. Sibiriak¹⁴⁶, S. Siddhanta⁵⁴, T. Siemiarz⁸², T.F. Silva¹¹³,
 D. Silvermyr⁷⁸, T. Simantathammakul¹⁰⁸, R. Simeonov³⁹, B. Singh⁹⁴, B. Singh⁹⁸, K. Singh⁵⁰,
 R. Singh⁸³, R. Singh⁹⁴, R. Singh⁵⁰, S. Singh¹⁶, V.K. Singh¹³⁷, V. Singhal¹³⁷, T. Sinha¹⁰²,
 B. Sitar¹³, M. Sitta^{135,59}, T.B. Skaali²¹, G. Skorodumovs⁹⁷, M. Slupecki⁴⁶, N. Smirnov¹⁴²,
 R.J.M. Snellings⁶², E.H. Solheim²¹, J. Song¹⁷, C. Sonnabend^{35,100}, F. Soramel³⁰,
 A.B. Soto-herandez⁹¹, R. Spijkers⁸⁷, I. Sputowska¹¹⁰, J. Staa⁷⁸, J. Stachel⁹⁷, I. Stan⁶⁶,
 P.J. Steffanic¹²⁴, S.F. Stiefelmaier⁹⁷, D. Stocco¹⁰⁶, I. Storehaug²¹, P. Stratmann¹⁴⁰, S. Strazzi²⁸,
 A. Sturmiolo^{33,55}, C.P. Stylianidis⁸⁷, A.A.P. Suaide¹¹³, C. Suire¹³³, M. Sukhanov¹⁴⁶, M. Suljic³⁵,
 R. Sultanov¹⁴⁶, V. Sumberia⁹⁴, S. Sumowidagdo⁸⁵, S. Swain⁶⁴, I. Szarka¹³, M. Szymkowski¹³⁸,
 S.F. Taghavi⁹⁸, G. Tallepied¹⁰⁰, J. Takahashi¹¹⁴, G.J. Tambave⁸³, S. Tang⁶, Z. Tang¹²², J.D. Tapia
 Takaki¹²⁰, N. Tapus¹²⁸, L.A. Tarasovicova¹⁴⁰, M.G. Tarzila⁴⁸, G.F. Tassielli³⁴, A. Tauro³⁵, G. Tejada
 Muñoz⁴⁷, A. Telesca³⁵, L. Terlizzi²⁷, C. Terrevoli¹¹⁸, S. Thakur⁴, D. Thomas¹¹¹,
 A. Tikhonov¹⁴⁶, A.R. Timmins¹¹⁸, M. Tkacik¹⁰⁹, T. Tkacik¹⁰⁹, A. Toia⁶⁷, R. Tokumoto⁹⁵,
 K. Tomohiro⁹⁵, N. Topilskaya¹⁴⁶, M. Toppi⁵¹, T. Tork¹³³, V.V. Torres¹⁰⁶, A.G. Torres Ramos³⁴,
 A. Trifiró^{33,55}, A.S. Triolo^{35,33,55}, S. Tripathy⁵³, T. Tripathy⁴⁹, S. Trogolo³⁵, V. Trubnikov³,
 W.H. Trzaska¹¹⁹, T.P. Trzcinski¹³⁸, A. Tumkin¹⁴⁶, R. Turrisi⁵⁶, T.S. Tveter²¹, K. Ullaland²²,
 B. Ulukutlu⁹⁸, A. Uras¹³⁰, G.L. Usai²⁴, M. Vala⁴⁰, N. Valle²³, L.V.R. van Doremalen⁶², M. van
 Leeuwen⁸⁷, C.A. van Veen⁹⁷, R.J.G. van Weelden⁸⁷, P. Vande Vyvre³⁵, D. Varga¹⁴¹, Z. Varga¹⁴¹,
 M. Vasileiou⁸¹, A. Vasiliev¹⁴⁶, O. Vázquez Doce⁵¹, O. Vazquez Rueda¹¹⁸, V. Vechnin¹⁴⁶,
 E. Vercellin²⁷, S. Vergara Limón⁴⁷, R. Verma⁴⁹, L. Vermunt¹⁰⁰, R. Vértesi¹⁴¹, M. Verweij⁶²,
 L. Vickovic³⁶, Z. Vilakazi¹²⁵, O. Villalobos Baillie¹⁰³, A. Villani²⁶, A. Vinogradov¹⁴⁶, T. Virgili³¹,
 M.M.O. Virta¹¹⁹, V. Vislavicius⁷⁸, M. Viviani⁵⁸, A. Vodopyanov¹⁴⁷, B. Volkel³⁵, M.A. Völkl⁹⁷,
 K. Voloshin¹⁴⁶, S.A. Voloshin¹³⁹, G. Volpe³⁴, B. von Haller³⁵, I. Vorobyev⁹⁸, N. Vozniuk¹⁴⁶,
 J. Vrláková⁴⁰, J. Wan⁴², C. Wang⁴², D. Wang⁴², Y. Wang⁴², Y. Wang⁶, A. Wegrzynek³⁵,
 F.T. Weiglhofer⁴¹, S.C. Wenzel³⁵, J.P. Wessels¹⁴⁰, S.L. Weyhmler¹⁴², J. Wiechula⁶⁷, J. Wikne²¹,
 G. Wilk⁸², J. Wilkinson¹⁰⁰, G.A. Willems¹⁴⁰, B. Windelband⁹⁷, M. Winn¹³², J.R. Wright¹¹¹,
 W. Wu⁴², Y. Wu¹²², R. Xu⁶, A. Yadav⁴⁵, A.K. Yadav¹³⁷, S. Yalcin⁷⁵, Y. Yamaguchi⁹⁵, S. Yang²²,
 S. Yano⁹⁵, Z. Yin⁶, I.-K. Yoo¹⁷, J.H. Yoon⁶¹, H. Yu¹², S. Yuan²², A. Yuncu⁹⁷, V. Zaccolo²⁶,

C. Zampolli ³⁵, F. Zanone ⁹⁷, N. Zardoshti ³⁵, A. Zarochentsev ¹⁴⁶, P. Závada ⁶⁵, N. Zaviyalov¹⁴⁶, M. Zhalov ¹⁴⁶, B. Zhang ⁶, C. Zhang ¹³², L. Zhang ⁴², S. Zhang ⁴², X. Zhang ⁶, Y. Zhang¹²², Z. Zhang ⁶, M. Zhao ¹⁰, V. Zherebchevskii ¹⁴⁶, Y. Zhi¹⁰, D. Zhou ⁶, Y. Zhou ⁸⁶, J. Zhu ^{100,6}, Y. Zhu⁶, S.C. Zugeravel ⁵⁹, N. Zurlo ^{136,57}

Affiliation Notes

^I Also at: Max-Planck-Institut für Physik, Munich, Germany

^{II} Also at: Italian National Agency for New Technologies, Energy and Sustainable Economic Development (ENEA), Bologna, Italy

^{III} Also at: Dipartimento DET del Politecnico di Torino, Turin, Italy

^{IV} Also at: Department of Applied Physics, Aligarh Muslim University, Aligarh, India

^V Also at: Institute of Theoretical Physics, University of Wrocław, Poland

^{VI} Also at: An institution covered by a cooperation agreement with CERN

Collaboration Institutes

¹ A.I. Alikhanyan National Science Laboratory (Yerevan Physics Institute) Foundation, Yerevan, Armenia

² AGH University of Krakow, Cracow, Poland

³ Bogolyubov Institute for Theoretical Physics, National Academy of Sciences of Ukraine, Kiev, Ukraine

⁴ Bose Institute, Department of Physics and Centre for Astroparticle Physics and Space Science (CAPSS), Kolkata, India

⁵ California Polytechnic State University, San Luis Obispo, California, United States

⁶ Central China Normal University, Wuhan, China

⁷ Centro de Aplicaciones Tecnológicas y Desarrollo Nuclear (CEADEN), Havana, Cuba

⁸ Centro de Investigación y de Estudios Avanzados (CINVESTAV), Mexico City and Mérida, Mexico

⁹ Chicago State University, Chicago, Illinois, United States

¹⁰ China Institute of Atomic Energy, Beijing, China

¹¹ China University of Geosciences, Wuhan, China

¹² Chungbuk National University, Cheongju, Republic of Korea

¹³ Comenius University Bratislava, Faculty of Mathematics, Physics and Informatics, Bratislava, Slovak Republic

¹⁴ COMSATS University Islamabad, Islamabad, Pakistan

¹⁵ Creighton University, Omaha, Nebraska, United States

¹⁶ Department of Physics, Aligarh Muslim University, Aligarh, India

¹⁷ Department of Physics, Pusan National University, Pusan, Republic of Korea

¹⁸ Department of Physics, Sejong University, Seoul, Republic of Korea

¹⁹ Department of Physics, University of California, Berkeley, California, United States

²⁰ Department of Physics of North Carolina State University, Raleigh, North Carolina, United States

²¹ Department of Physics, University of Oslo, Oslo, Norway

²² Department of Physics and Technology, University of Bergen, Bergen, Norway

²³ Dipartimento di Fisica, Università di Pavia, Pavia, Italy

²⁴ Dipartimento di Fisica dell'Università and Sezione INFN, Cagliari, Italy

²⁵ Dipartimento di Fisica dell'Università and Sezione INFN, Pisa, Italy

²⁶ Dipartimento di Fisica dell'Università and Sezione INFN, Trieste, Italy

²⁷ Dipartimento di Fisica dell'Università and Sezione INFN, Turin, Italy

²⁸ Dipartimento di Fisica e Astronomia dell'Università and Sezione INFN, Bologna, Italy

²⁹ Dipartimento di Fisica e Astronomia dell'Università and Sezione INFN, Catania, Italy

³⁰ Dipartimento di Fisica e Astronomia dell'Università and Sezione INFN, Padova, Italy

³¹ Dipartimento di Fisica 'E.R. Caianiello' dell'Università and Gruppo Collegato INFN, Salerno, Italy

³² Dipartimento DISAT del Politecnico and Sezione INFN, Turin, Italy

³³ Dipartimento di Scienze MIFT, Università di Messina, Messina, Italy

³⁴ Dipartimento Interateneo di Fisica 'M. Merlin' and Sezione INFN, Bari, Italy

³⁵ European Organization for Nuclear Research (CERN), Geneva, Switzerland

³⁶ Faculty of Electrical Engineering, Mechanical Engineering and Naval Architecture, University of Split, Split, Croatia

³⁷ Faculty of Engineering and Science, Western Norway University of Applied Sciences, Bergen, Norway

- ³⁸ Faculty of Nuclear Sciences and Physical Engineering, Czech Technical University in Prague, Prague, Czech Republic
- ³⁹ Faculty of Physics, Sofia University, Sofia, Bulgaria
- ⁴⁰ Faculty of Science, P.J. Šafárik University, Košice, Slovak Republic
- ⁴¹ Frankfurt Institute for Advanced Studies, Johann Wolfgang Goethe-Universität Frankfurt, Frankfurt, Germany
- ⁴² Fudan University, Shanghai, China
- ⁴³ Gangneung-Wonju National University, Gangneung, Republic of Korea
- ⁴⁴ Gauhati University, Department of Physics, Guwahati, India
- ⁴⁵ Helmholtz-Institut für Strahlen- und Kernphysik, Rheinische Friedrich-Wilhelms-Universität Bonn, Bonn, Germany
- ⁴⁶ Helsinki Institute of Physics (HIP), Helsinki, Finland
- ⁴⁷ High Energy Physics Group, Universidad Autónoma de Puebla, Puebla, Mexico
- ⁴⁸ Horia Hulubei National Institute of Physics and Nuclear Engineering, Bucharest, Romania
- ⁴⁹ Indian Institute of Technology Bombay (IIT), Mumbai, India
- ⁵⁰ Indian Institute of Technology Indore, Indore, India
- ⁵¹ INFN, Laboratori Nazionali di Frascati, Frascati, Italy
- ⁵² INFN, Sezione di Bari, Bari, Italy
- ⁵³ INFN, Sezione di Bologna, Bologna, Italy
- ⁵⁴ INFN, Sezione di Cagliari, Cagliari, Italy
- ⁵⁵ INFN, Sezione di Catania, Catania, Italy
- ⁵⁶ INFN, Sezione di Padova, Padova, Italy
- ⁵⁷ INFN, Sezione di Pavia, Pavia, Italy
- ⁵⁸ INFN, Sezione di Pisa, Pisa, Italy
- ⁵⁹ INFN, Sezione di Torino, Turin, Italy
- ⁶⁰ INFN, Sezione di Trieste, Trieste, Italy
- ⁶¹ Inha University, Incheon, Republic of Korea
- ⁶² Institute for Gravitational and Subatomic Physics (GRASP), Utrecht University/Nikhef, Utrecht, Netherlands
- ⁶³ Institute of Experimental Physics, Slovak Academy of Sciences, Košice, Slovak Republic
- ⁶⁴ Institute of Physics, Homi Bhabha National Institute, Bhubaneswar, India
- ⁶⁵ Institute of Physics of the Czech Academy of Sciences, Prague, Czech Republic
- ⁶⁶ Institute of Space Science (ISS), Bucharest, Romania
- ⁶⁷ Institut für Kernphysik, Johann Wolfgang Goethe-Universität Frankfurt, Frankfurt, Germany
- ⁶⁸ Instituto de Ciencias Nucleares, Universidad Nacional Autónoma de México, Mexico City, Mexico
- ⁶⁹ Instituto de Física, Universidade Federal do Rio Grande do Sul (UFRGS), Porto Alegre, Brazil
- ⁷⁰ Instituto de Física, Universidad Nacional Autónoma de México, Mexico City, Mexico
- ⁷¹ iThemba LABS, National Research Foundation, Somerset West, South Africa
- ⁷² Jeonbuk National University, Jeonju, Republic of Korea
- ⁷³ Johann-Wolfgang-Goethe Universität Frankfurt Institut für Informatik, Fachbereich Informatik und Mathematik, Frankfurt, Germany
- ⁷⁴ Korea Institute of Science and Technology Information, Daejeon, Republic of Korea
- ⁷⁵ KTO Karatay University, Konya, Turkey
- ⁷⁶ Laboratoire de Physique Subatomique et de Cosmologie, Université Grenoble-Alpes, CNRS-IN2P3, Grenoble, France
- ⁷⁷ Lawrence Berkeley National Laboratory, Berkeley, California, United States
- ⁷⁸ Lund University Department of Physics, Division of Particle Physics, Lund, Sweden
- ⁷⁹ Nagasaki Institute of Applied Science, Nagasaki, Japan
- ⁸⁰ Nara Women's University (NWU), Nara, Japan
- ⁸¹ National and Kapodistrian University of Athens, School of Science, Department of Physics, Athens, Greece
- ⁸² National Centre for Nuclear Research, Warsaw, Poland
- ⁸³ National Institute of Science Education and Research, Homi Bhabha National Institute, Jatni, India
- ⁸⁴ National Nuclear Research Center, Baku, Azerbaijan
- ⁸⁵ National Research and Innovation Agency - BRIN, Jakarta, Indonesia
- ⁸⁶ Niels Bohr Institute, University of Copenhagen, Copenhagen, Denmark
- ⁸⁷ Nikhef, National institute for subatomic physics, Amsterdam, Netherlands
- ⁸⁸ Nuclear Physics Group, STFC Daresbury Laboratory, Daresbury, United Kingdom
- ⁸⁹ Nuclear Physics Institute of the Czech Academy of Sciences, Husinec-Řež, Czech Republic

- ⁹⁰ Oak Ridge National Laboratory, Oak Ridge, Tennessee, United States
- ⁹¹ Ohio State University, Columbus, Ohio, United States
- ⁹² Physics department, Faculty of science, University of Zagreb, Zagreb, Croatia
- ⁹³ Physics Department, Panjab University, Chandigarh, India
- ⁹⁴ Physics Department, University of Jammu, Jammu, India
- ⁹⁵ Physics Program and International Institute for Sustainability with Knotted Chiral Meta Matter (SKCM2), Hiroshima University, Hiroshima, Japan
- ⁹⁶ Physikalisches Institut, Eberhard-Karls-Universität Tübingen, Tübingen, Germany
- ⁹⁷ Physikalisches Institut, Ruprecht-Karls-Universität Heidelberg, Heidelberg, Germany
- ⁹⁸ Physik Department, Technische Universität München, Munich, Germany
- ⁹⁹ Politecnico di Bari and Sezione INFN, Bari, Italy
- ¹⁰⁰ Research Division and ExtreMe Matter Institute EMMI, GSI Helmholtzzentrum für Schwerionenforschung GmbH, Darmstadt, Germany
- ¹⁰¹ Saga University, Saga, Japan
- ¹⁰² Saha Institute of Nuclear Physics, Homi Bhabha National Institute, Kolkata, India
- ¹⁰³ School of Physics and Astronomy, University of Birmingham, Birmingham, United Kingdom
- ¹⁰⁴ Sección Física, Departamento de Ciencias, Pontificia Universidad Católica del Perú, Lima, Peru
- ¹⁰⁵ Stefan Meyer Institut für Subatomare Physik (SMI), Vienna, Austria
- ¹⁰⁶ SUBATECH, IMT Atlantique, Nantes Université, CNRS-IN2P3, Nantes, France
- ¹⁰⁷ Sungkyunkwan University, Suwon City, Republic of Korea
- ¹⁰⁸ Suranaree University of Technology, Nakhon Ratchasima, Thailand
- ¹⁰⁹ Technical University of Košice, Košice, Slovak Republic
- ¹¹⁰ The Henryk Niewodniczanski Institute of Nuclear Physics, Polish Academy of Sciences, Cracow, Poland
- ¹¹¹ The University of Texas at Austin, Austin, Texas, United States
- ¹¹² Universidad Autónoma de Sinaloa, Culiacán, Mexico
- ¹¹³ Universidade de São Paulo (USP), São Paulo, Brazil
- ¹¹⁴ Universidade Estadual de Campinas (UNICAMP), Campinas, Brazil
- ¹¹⁵ Universidade Federal do ABC, Santo Andre, Brazil
- ¹¹⁶ University of Cape Town, Cape Town, South Africa
- ¹¹⁷ University of Derby, Derby, United Kingdom
- ¹¹⁸ University of Houston, Houston, Texas, United States
- ¹¹⁹ University of Jyväskylä, Jyväskylä, Finland
- ¹²⁰ University of Kansas, Lawrence, Kansas, United States
- ¹²¹ University of Liverpool, Liverpool, United Kingdom
- ¹²² University of Science and Technology of China, Hefei, China
- ¹²³ University of South-Eastern Norway, Kongsberg, Norway
- ¹²⁴ University of Tennessee, Knoxville, Tennessee, United States
- ¹²⁵ University of the Witwatersrand, Johannesburg, South Africa
- ¹²⁶ University of Tokyo, Tokyo, Japan
- ¹²⁷ University of Tsukuba, Tsukuba, Japan
- ¹²⁸ University Politehnica of Bucharest, Bucharest, Romania
- ¹²⁹ Université Clermont Auvergne, CNRS/IN2P3, LPC, Clermont-Ferrand, France
- ¹³⁰ Université de Lyon, CNRS/IN2P3, Institut de Physique des 2 Infinis de Lyon, Lyon, France
- ¹³¹ Université de Strasbourg, CNRS, IPHC UMR 7178, F-67000 Strasbourg, France, Strasbourg, France
- ¹³² Université Paris-Saclay, Centre d'Etudes de Saclay (CEA), IRFU, Département de Physique Nucléaire (DPhN), Saclay, France
- ¹³³ Université Paris-Saclay, CNRS/IN2P3, IJCLab, Orsay, France
- ¹³⁴ Università degli Studi di Foggia, Foggia, Italy
- ¹³⁵ Università del Piemonte Orientale, Vercelli, Italy
- ¹³⁶ Università di Brescia, Brescia, Italy
- ¹³⁷ Variable Energy Cyclotron Centre, Homi Bhabha National Institute, Kolkata, India
- ¹³⁸ Warsaw University of Technology, Warsaw, Poland
- ¹³⁹ Wayne State University, Detroit, Michigan, United States
- ¹⁴⁰ Westfälische Wilhelms-Universität Münster, Institut für Kernphysik, Münster, Germany
- ¹⁴¹ Wigner Research Centre for Physics, Budapest, Hungary
- ¹⁴² Yale University, New Haven, Connecticut, United States

¹⁴³ Yonsei University, Seoul, Republic of Korea

¹⁴⁴ Yukawa Institute for Theoretical Physics, Kyoto University, Kyoto, Japan

¹⁴⁵ Zentrum für Technologie und Transfer (ZTT), Worms, Germany

¹⁴⁶ Affiliated with an institute covered by a cooperation agreement with CERN

¹⁴⁷ Affiliated with an international laboratory covered by a cooperation agreement with CERN.